

Review

Surface Modification of Screen-Printed Carbon Electrodes

Naila Haroon  and Keith J. Stine * 

Department of Chemistry and Biochemistry, University of Missouri—Saint Louis, Saint Louis, MO 63121, USA; nhymm@umsl.edu

* Correspondence: kstine@umsl.edu

Abstract

SPCEs are crucial for electrochemical sensing because of their portability, low cost, disposability, and ease of mass production. This study details their manufacture, surface modifications, electrochemical characterization, and use in chemical and biosensing. SPCEs integrate working, reference, and counter electrodes on PVC or polyester substrates for compact sensor design. Surface modifications, such as plasma treatment (O₂, Ar), nanomaterial addition (AuNPs, GO, CNTs), polymer coatings, and MIPs, enhance performance. These changes improve sensitivity, selectivity, stability, and electron transport. Electrochemical methods such as CV, DPV, SWV, and EIS detect analytes, including biomolecules (glucose, dopamine, and pathogens) and heavy metals (Pb²⁺, As³⁺). Their applications include healthcare diagnostics, environmental monitoring, and food safety. Modified SPCEs enable rapid on-site analysis and offer strong potential to transform our understanding of the physical world.

Keywords: SPCE; electrochemical techniques; electrochemical sensors; biosensors; FIA; modification; nanomaterials; molecularly imprinted polymer

1. Introduction

According to the International Union of Pure and Applied Chemistry (IUPAC), a chemical sensor is “a device that turns chemical data into a signal that can be used for analysis.” Most chemical sensors have a surface designed to have some selectivity for the analyte that is on top of a physicochemical transducer. The surface may be physically modified or chemically modified with receptors or macromolecules that interact with the analyte in a specific manner. Biosensors use biological receptors, including DNA, antibodies, and enzymes. The receptor converts analyte recognition into a predetermined output signal. To avoid false-positive results, sensors must be highly selective for the analyte in the presence of other species that could interfere. In electrochemical sensors, the transducer converts the transfer of charge due to oxidation or reduction in the analyte into a readable signal. Chemical sensors and biosensors can be catalytic or affinity-based. Affinity-based devices require specific recognition of the analyte by the receptor to generate a signal. These binding events include aptamers binding to their targets, antibodies binding to their antigens, binding of complementary DNA strands, and host–guest supramolecular interactions. In contrast, catalytic sensors use catalytic activity, generally that of enzymes, to produce a signal. Depending on the transducer, recognition events can be observed, measured, or detected using optical, gravimetric, or electrochemical measurements. Electrochemical sensing is a highly effective method for detecting a wide range of chemical species. It provides elevated sensitivity, rapid reaction, ease of use, real-time monitoring, and the potential for downsizing [1–5].



Academic Editor: Giorgos Skordaris

Received: 1 September 2025

Revised: 1 October 2025

Accepted: 7 October 2025

Published: 9 October 2025

Citation: Haroon, N.; Stine, K.J. Surface Modification of Screen-Printed Carbon Electrodes. *Coatings* **2025**, *15*, 1182. <https://doi.org/10.3390/coatings15101182>

Copyright: © 2025 by the authors. Licensee MDPI, Basel, Switzerland. This article is an open access article distributed under the terms and conditions of the Creative Commons Attribution (CC BY) license (<https://creativecommons.org/licenses/by/4.0/>).

Biosensors provide precise electrical signals, allowing them to measure the concentration of biological analytes. Therefore, electrochemical methods can be used to their full potential in biological contexts. The low price and short reaction time of these sensors make them useful in various contexts, including healthcare, diagnostics, environmental monitoring, and clinical analysis. Several research projects have focused on developing biosensors that offer point-of-care diagnostics, especially for resource-constrained environments, owing to their low cost, portability, ease of use, and capacity to offer real-time remote healthcare monitoring. Electrochemical biosensors are ideal for point-of-care (POC) quantitative detection of catalytic and affinity biorecognition events because they can directly transform biological events into electrical signals and are easy to integrate with microelectronics [6–9].

A growing number of electrochemical and biosensors are developed each year. These sensors are utilized in the pharmaceutical, biological, industrial, and environmental analytical domains for in situ monitoring and point-of-care testing. A disposable electrode is essential for in situ monitoring and point-of-care analysis. Wearable electronics have recently gained popularity because they are portable and can provide rapid results. Reliable and efficient methods of mass production are required to meet this demand. Screen printing is a simple, inexpensive, and versatile technique. This additive manufacturing technique is held in high regard for these reasons. The fundamental layout requires the squeegee for up-and-down printing, meshwork to house the pattern, and paste(s) for printing. Since the 1990s, screen-printed electrodes (SPEs) have served as disposable point-of-care diagnostic tools for designing electrochemical sensors that comply with the requisite criteria. Screen printing the electrode onto a substrate facilitates miniaturization, cost-effectiveness, and portability of the sensor by integrating the working, reference, and counter electrodes. SPEs are conducive to mass manufacturing because of their simplicity in fabrication and reduced complexity of the sensor design [10–13].

Numerous types of SPEs have been developed, with carbon-based electrodes being among the most investigated owing to their immense applications in chemical and biochemical sensing. Electrochemical sensors constructed using SPCE are widely favored because of the several advantageous properties of carbon (i.e., structural, natural, and physicochemical), including ease of operation, affordability, disposability, inertness, portability, minimal background current, simplicity, easy chemical modification, and extensive potential window. An SPCE comprises a carbon working electrode, a reference electrode, and a counter electrode, all of which are integrated onto a substrate [14–18].

In comparing the performance of SPCE and modified SPCE, there are numerous parameters to be considered. The effect of the modification on the limit of detection, linear range, and selectivity is important for the sensor performance. The stability of the modified electrode under storage and under repeated usage is of significant concern. Reproducibility of response for electrodes modified in the same manner is a significant issue. The successful modification of SPCE will generally enhance the electron transport from the redox process involved in detection, and this can be evidenced by a reduction in the charge transfer resistance as measured by EIS. The SPCE modification may also increase the available surface area of the electrode. The uniformity of the modification is important, as well as any introduced porosity or roughness. For practical considerations, the complexity and cost of the modification process should be considered, and if the SPCE is used in vivo, then biocompatibility is of concern. Since SPCEs are meant to be disposable, the impact of their disposal on the environment has led to a rise in interest in making them biodegradable and using manufacturing processes of reduced environmental impact.

The first step in fabricating an SPCE is to prepare a conductive carbon-based ink for the working electrode. Carbon materials, such as graphite or carbon black, as well as

carbon-based nanomaterials such as graphene or carbon nanofibers, can also be used as the main component of the ink for the working electrode. Single-walled or multi-walled carbon nanotubes may also be used to provide high conductivity and improved performance. Silver chloride ink is most commonly used to make the reference electrode, although the reference electrode can also be carbon or silver. The counter electrode is most commonly made from a carbon-based ink, although silver or platinum ink can also be used.

Conductive inks for making SPCEs contain carbon, organic solvents, binding pastes, and other chemicals that confer useful properties. The success of SPCE fabrication is influenced by multiple factors, including the composition of the conductive ink, the substrate used, and the fabrication technique employed. The ink composition must include a conductive material that exhibits high conductivity. Various carbon-based materials, such as graphite, graphene, and carbon nanotubes, have potential for the fabrication of SPCE. Additional materials that are crucial for the properties of conductive inks include binders and solvents. Binders improve ink properties, such as viscosity, homogeneity, and adhesion to the substrate. The solvent must effectively disperse both the conductive material and binder to achieve a uniform mixture. Additionally, the properties of the conductive ink must be compatible with both the substrate and the fabrication technique employed. The literature review indicates that the predominant techniques for SPCE fabrication are screen and inkjet printing. Both printing technologies can produce electrodes that meet the specifications for electrochemical measurements and sensing [14,19,20].

2. Structural Features of SPCE

In one report, CorelDraw X7 software was used with the template of the widely available SPCE from Metrohm as a guide to create a template for a homemade SPCE. A printer with Camel glossy sticker paper made using the cutting sticker method was used to create the template pattern. A paintbrush was used to apply the conductive ink on the polyvinyl chloride (PVC) paper base. First, dichloromethane (DCM) was used to clean the PVC paper before it was used. Subsequently, the SPCE pattern was placed on top of the PVC paper base. Graphite ink was then applied to the PVC paper base using a brush, and the SPCE pattern was used to guide the process. It was necessary to perform this step twice to achieve a smooth surface. To ensure that the graphite ink adhered well to the PVC base, the SPCE was baked in an oven at 50 °C for 5 min. Subsequently, silver ink was used to make the RE, which was left to dry for 5 min. To obtain the SPCE, the template was removed from the PVC paper base. Then, paraffin wax was placed on top of the homemade SPCE to keep the electrodes in place. Additionally, copper foil was placed on the reference electrode (RE), working electrode (WE), and counter electrode (CE) connection routes of the SPCE, as shown in Figure 1 [19].

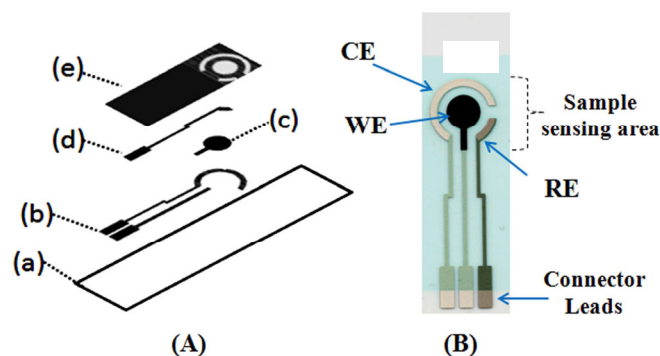


Figure 1. (A) Scheme for screen printing of silver/carbon screen-printed electrode (S/C-SPE), (a) polyester substrate, (b) silver track, (c) carbon layer, (d) silver/silver chloride track, and (e) insulating

layer; (B) screen printed silver/carbon electrode (S/C-SPE). Reproduced from reference [21] with permission from Elsevier, copyright 2018.

The SPE fabrication process is quick and allows for the efficient and consistent production of small, low-cost electrodes that are used only once. Carbon and metallic inks are the most common types of inks or pastes (viscous fluids) used for printing electrodes. A blade (3–10 Pa at a shear rate of 230 s^{-1}) is used on a mesh screen on the substrate, which is usually ceramic or plastic, such as polyvinylchloride and polycarbonate. The mesh screen has a specific pattern that shows how the electrodes are shaped and measured in the simulation. Because of the general analytical function and trading value of making sensors, the paste formulation is mostly a business secret for commercial SPCEs. Carbon-containing materials such as graphite, fullerene, graphene (Gr), carbon nanotubes (CNTs), and similar materials are commonly used for making WEs because they perform well in electrochemical tests and are inexpensive. They are also chemically stable, have high conductivity, are easy to modify, have wide potential windows, and exhibit low background currents. In addition to carbon inks, other conductive inks have also been widely used. In addition, Au ink is the most popular because it facilitates the modification of the protein surface using self-assembled monolayer (SAM) formation, as it resembles thiol moieties. It is worth mentioning that there are other SPEs with a WE, as shown in Figure 2, made of metallic inks, such as gold (Au), silver (Ag), platinum (Pt), or palladium (Pd). However, these are rarely used and are only suitable for certain tasks. Silver or silver/silver chloride inks are often used for RE building. This type of RE is called “quasi-reference” or “pseudo-reference” because its potential is not stable like an ideal RE would be. Therefore, the potential is not considered as accurate and repeatable as for ideal REs, such as the Ag/AgCl electrode [22].

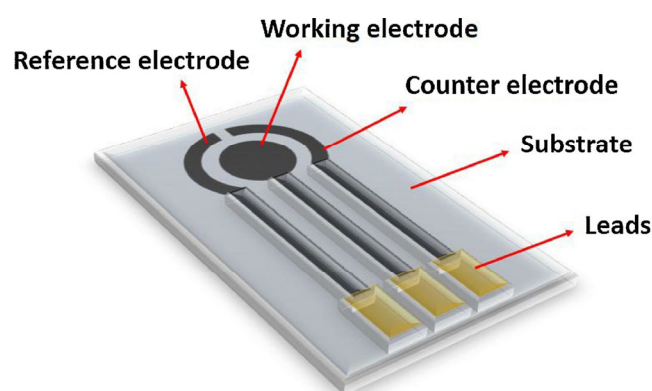


Figure 2. Schematic representation of a screen-printed electrode. Reproduced from ref. [23], with permission from Elsevier, copyright 2018.

The chemical composition of the ink is important for electrochemical applications. Several companies have patents on their ink formula and the structure of SPEs; therefore, customers are unaware of the details. By changing the number of particles loaded, the composition of the ink can be changed. This has a significant impact on the electron transfer process and the performance of the designed SPEs. To adhere the paste to the base, glues such as ethylene glycol, cellulose acetate, resin, or cyclohexanone are added. The sensitivity, specificity, and signal-to-noise ratio (S/N) can be improved by mixing the ingredients. In some cases, it has been shown that the ink contains silver, platinum powder, or even gold to boost the electrochemical signal for biological or physical interactions.

In summary, building an SPE involves several steps:

- (1) Choosing the mesh or screen design to determine the SPE size and shape is important.
- (2) Obtaining the correct conductive inks and materials for the substrate.

- (3) A thin film was made by layer-by-layer (LBL) deposition to choose the inks for the substrate.
- (4) The film was dried using hot air and IR radiation and cured to set the ink. Analytical tests can be performed after placing an insulating material over the electrical circuits. This is achieved by placing a single drop of the sample (analyte) solution on the SPE surface [22].

The three-electrode system comprised a reference, working, and counter electrode. The silver reference electrode joins the carbon counter and working electrodes, whereas the dielectric layers are delineated by distinct screen patterns, as illustrated in the figure. The screens can simultaneously manufacture 12 electrochemical sensors [24].

Unmodified SPCEs are subject to a number of limitations. Use of different inks and printing conditions will introduce variability. The surface morphology of SPCEs is rough and porous, and these properties can vary with the printing conditions. Unmodified SPCEs are prone to surface fouling, and fouling will decrease the electrode response. The mechanical stability of the printed electrode on the substrate is also a potential problem, especially in harsher environments. Unmodified SPCEs do not have especially efficient electron transfer kinetics, resulting in lower currents and broader peaks. One of the motivations for seeking to modify them is to increase the electron transfer efficiency.

Commercial Platforms for Working with SPCEs

There are a number of commercial sources for the acquisition of pre-made SPCEs and modified SPCEs, and these companies generally also provide other accessories such as flow cells and specialized potentiostats. Three of the major commercial platforms are Metrohm-Dropsens (<https://metrohm-dropsens.com/>, Spain, accessed on 20 September 2025), Palmsens (<https://www.palmsens.com/>, Netherlands, accessed on 20 September 2025), and Micrux (<https://www.micruxfluidic.com/>, Spain, accessed on 20 September 2025), all of which have distributors in multiple countries. Metrohm-Dropsens offers SPCEs on a ceramic substrate of dimensions 3.38 cm × 1.02 cm × 0.05 cm with a 0.40 cm diameter working electrode in the middle of the strip. A choice of Ag or Ag/AgCl reference and of either C or Pt auxiliary electrodes is available. SPCEs with 2, 4, and 8 working electrodes are available. The eight-working-electrode version has the working electrodes arranged in a circle near the middle of the strip. For all of the numbers of working electrodes, connectors are available so that these SPCEs can be interfaced to a potentiostat. A special 96-well ELISA plate with a printed carbon electrode in each well is available, with independent auxiliary and reference electrodes and gold contacts at the bottom of the well plate for attachment to a special connector box to use together with a potentiostat. This well plate uses 300–400 mL volumes and is intended for bioassay development. An option for an SPCE with the working electrode placed closer to the end of the strip for use in solution, instead of applying small volumes to the working electrode(s), is available. Numerous modified SPCEs are available, including carbon nanofibers, multi-walled carbon nanotubes, graphene, and gold nanoparticles. Special modifications, such as metal phthalocyanines as oxidase enzyme mediators, are available to facilitate the detection of hydrogen peroxide. Flow cells compatible with SPCEs, including wall-jet flow cells, are also available. A handheld electrochemical reader is available that would be suitable for field work, along with other small-footprint potentiostats, bipotentiostats, and multipotentiostats. Palmsens also provides an assortment of SPCEs flow cells, with some choices of substrate including ceramic, polyester, and polyimide. SPCEs modified with the enzymes acetylcholinesterase and glucose oxidase are available. A wearable patch for tracking sweat or metabolites using SPCE is sold and can be used with a Sensit wearable potentiostat capable of most electrochemical methods, from which data can be transferred to a PC. The Sensit has

recently been used to measure lactate in sweat using a wearable biosensor integrated into an armband [25]. Micrux has an all-in-one cell for use with SPCEs in either batch or flow mode, microfluidic platforms, and other accessories such as syringes and peristaltic pumps. Zenor R&D (<https://www.zensorrd.com/>, Taiwan, accessed on 20 September 2025) offers finger-sized single and multipotentiostats into which an SPE can be simply inserted and from which the data can be transferred to a smartphone. The company also offers flexible SPE on a polyimide substrate that can be bent or wrapped, which is attractive for the development of wearable sensors. The availability of small, portable, and wireless potentiostats with data display and analysis on laptops and cell phones makes the field and point-of-care use of SPCEs more feasible and attractive. Directly ready-to-use electrochemical biosensors based on SPCEs, including ones that are wearable, are also available (<https://www.zimmerpeacock.com/products/>, accessed on 20 September 2025). Researchers have the option to fabricate their own SPCE in-house using their own substrates and either purchased or home-made inks, or they can purchase bare or modified SPCEs suitable for their specialized applications, or pre-made, ready-to-use sensors. Eastprint (<https://www.eastprint.com/electrodes-biosensors/>, accessed on 20 September 2025) is another company specializing in printed electronics, including SPCEs.

3. Electrochemical Methods Used for SPCE Characterization and Application

Various electrochemical methods are used for the modification, cleaning, pretreatment, and characterization of SPCEs, as well as for analyte detection. The electrochemical properties of the SPCE, such as reversibility, electron transfer kinetics, potential window, and charge transfer resistance, have been studied using cyclic voltammetry (CV), linear sweep voltammetry (LSV), chronoamperometry (CA), electrochemical impedance spectroscopy (EIS), differential pulse voltammetry (DPV), and square wave voltammetry (SWV). EIS is especially useful for characterizing modified electrodes since modification is used to reduce the charge transfer resistance (R_{ct}) and enhance the sensor response. These methods are also important for studying electrode stability, resistance to fouling, selectivity in the presence of interferents, and repeatability. All these methods have found applications in analyte detection, especially CA, DPV, and SWV [26]. Flow injection analysis uses continuous analyte flow to provide rapid and reproducible measurements coupled with other electrochemical techniques.

3.1. Cyclic Voltammetry (CV)

CV is a potential sweep technique, and the results depend on the analyte redox properties and concentration, and additional factors, such as the electrolyte and electrode, and contain both kinetic and thermodynamic information. The starting potential is often set to the (open circuit/resting/equilibrium) potential, at which there is no visible external current flow. The potential is then scanned at a steady rate in one direction, followed by the opposite sweep direction after the reversal potential [27,28]. There is no need for stirring in the CV experiment, and diffusion plays an important role in mass transfer. The diffusion layer is the area close to the electrode surface that changes because of electron flow and diffusion. Furthermore, once the current reaches its peak, it drops back down towards a steady state value, giving the typical “duck” form for a reversible cyclic voltammogram. This current reaction happens when redox-active species are removed from the diffusion layer. The steady-state current is determined by the extent to which the bulk solution penetrates the diffusion layer [29,30]. It is a prevalent electrochemical detection technique that serves not only for the surface characterization of electrodes and detection but also as an exceptional approach for the modification of electrodes. The fundamental and most

commonly employed CV method is also used for the modification and characterization of electrodes in electrochemical measurements [31]. This technique can be employed to investigate the characteristics of SPCEs, their potential ranges, the intensities of the background currents, and the prevalence of chemical reactions to investigate redox reactions [32]. Modification of the SPCE surface can affect the diffusion rate and this can affect the linear range for analyte detection.

Rosello et al. investigated an efficient method for distinguishing beers, making use of CV with a commercial SPCE. The data were subjected to partial least squares discriminant analysis (PLS DA) and support vector machine discriminant analysis (SVM DA), which helped with sorting the beers into groups. Partial least squares (PLS) and artificial neural networks (ANN) can also be used on CV data from drinks to estimate the alcohol level [33]. Herbei et al. developed coated SPEs using nanocomposite chitosan-based zinc oxide (ZnO), silver (Ag), and Ag-ZnO nanoparticles for future use in cancer tumor biomarker detection. The electrochemical behavior of a 10 mM potassium ferrocyanide in a 0.1 M buffer solution redox system was evaluated by CV at scan rates from 0.02 to 0.7 V s⁻¹. The scan rate affected the anodic and cathodic peak currents. Both anodic and cathodic currents were higher at 0.1 V s⁻¹ ($I_a = 22 \mu\text{A}$ and $I_c = -25 \mu\text{A}$) than at 0.06 V s⁻¹ ($I_a = 10 \mu\text{A}$ and $I_c = -14 \mu\text{A}$) [34]. Mashat et al. developed multi-walled carbon nanotubes (MWCNT) with zinc oxide nanoparticles (ZnO NP) and molecularly imprinted polymer (MIP) on an SPCE to make an electrochemical sensor that was enzyme free for sensing glucose, and used CV to study different factors like sensitivity, selectivity, and LOD [35].

In another study, Jazi et al. modified the SPCE surface to create a non-enzymatic sensor for glucose detection. The idea behind the platform was to improve biomolecule detection using portable and disposable electrode architecture. The SPCE carbon surface was engraved with circular lines using a pulsed laser. Consequently, the surface of the laser-engraved screen-printed carbon electrode (LSPCE) was coated with MWCNTs and ZnO nanoparticles using drop-casting and radio frequency (RF) sputtering, respectively. CV was used to study the electrochemical performance and electrochemical behavior of the modified electrodes. A linear range of 1–10 mM with a detection limit of 0.43 mM for glucose was achieved [36].

3.2. Differential Pulse Voltammetry (DPV)

DPV is a method that provides high sensitivity and reduced background currents [36]. In DPV, the potential is increased in a staircase ramp, and a potential pulse is applied at the end of each step. Current is measured just before the pulse and near the end of the pulse, and the difference between these two currents is recorded. Given that capacitive currents due to electric double layer rearrangement decay quickly, their contribution is minimized by taking the current difference between that at the end of the pulse and at the beginning. The current due to the Faradaic processes of interest is thus made more prominent, and the difference current is plotted vs. potential. The peak current will occur near the redox potential of the analyte, and the peak current will be proportional to concentration [18,37,38].

Tysczuk-Rotko et al. used DPV and an electrochemically activated screen-printed carbon electrode (aSPCE) to detect ibuprofen (IBP). The SPCE was activated by five CV cycles from 0 to 2.0 V at 100 mV s⁻¹ in 0.1 M NaOH. Activation improved the DPV response. The procedure also gave a wide linear range up to 500 mM, low LOD (0.059 mM) and LOQ, selectivity, good IBP signal repeatability and reproducibility from electrode to electrode, low reagent use, easy sample preparation, and low cost for IBP analysis [39]. A quick and inexpensive method for detecting the antibiotic sulfamethoxazole (SMX) using DPV was developed using SPCE performed in an acetate buffer with a pH of 5.5. This resulted in

a detection limit of $15 \mu\text{g L}^{-1}$, a linear range of $50\text{--}600 \mu\text{g L}^{-1}$, and good repeatability (1.1%) and reproducibility (2.5%). The method worked well for testing in samples of spiked tap water, with a very high level of repeatability (0.4%) and good accuracy (95.2% recovery) [40].

Jirasirichote et al. used SPCE modified with graphene oxide (GO) and gold nanoparticles (AuNPs) for carbofuran detection using DPV. Analysis factors such as the working solution pH and the amount of GO and AuNPs on the electrode surface were optimized using the central composite design (CCD) method. The method showed a wide linear range of $1\text{--}250 \mu\text{M}$, with limits of detection and quantification of 0.22 and $0.72 \mu\text{M}$, respectively, for analyte measurement. Additionally, cucumber and rice samples were tested for carbofuran [41]. Ramaraj et al. recorded the superior electrochemical features of Fe-treated MoSe_2 using different methods, including simple chemical synthesis (C- FeMoSe_2), microwave-assisted synthesis (M- FeMoSe_2), and the hydrothermal method (H- FeMoSe_2) for MES electrochemical sensors. Among these methods, the H- FeMoSe_2 -modified SPCE (H- FeMoSe_2 /SPCE) had better electrochemical properties, with 0.44 and 0.57 times less charge transfer resistance and 0.46 and 1.28 times higher oxidation current response of MES than the M- FeMoSe_2 and C- FeMoSe_2 modified electrodes, respectively. The DPV method showed a very low detection limit of 0.8 nM and a high level of sensitivity ($0.24 \text{ mA mM}^{-1} \text{ cm}^{-2}$) [42].

3.3. Square Wave Voltammetry (SWV)

SWV is one of the most sophisticated, adaptable, and accurate methods within the pulse voltammetric category for the direct assessment of analyte concentrations. The waveform consists of a square-wave superimposed on a staircase. A normal SW voltammogram has three I–E curves: two can be measured directly (forward and reverse pulse), and a difference current is taken as the forward current minus the reverse current. SWV difference current has enhanced sensitivity to Faradaic processes, much like DPV. SWV combines the benefits of cyclic and pulse voltammetry as a tool for studying mechanisms with high sensitivity, usually higher than DPV, and has been used in the past few years for the fabrication of various highly sensitive biosensors and electrochemical sensors. SWV provides both kinetic and mechanistic information about electrodes [43–49].

Ji et al. created an SWV-based device that works on smartphones and combined it with SPGE to determine norepinephrine in real time. The detector could be used to excite the electrode and measure the current, and the smartphone could be used to send commands, record data, and display the results. The SPGE had good electrical and chemical qualities, was stable over time, and was very sensitive. There was a bigger difference between the slopes of SPGE and SPCE. As little as $0.265 \mu\text{M}$ of norepinephrine could be detected by the SPGE system on the smartphone. This means that the SPGE method could be used for point-of-care testing to find biochemical molecules quickly and accurately [50]. Newair et al. conducted an analysis of polyphenols in French red wines utilizing SWV. Voltammetric tests were performed on glassy carbon electrodes (GCEs) and disposable SPCEs, both in their untreated state and modified with single- and multi-walled carbon nanotubes. The SWCNTs-SPCE exhibited superior voltammetric measurement of polyphenols in red wine samples, facilitating the use of disposable electrodes for experimentation. The voltammograms exhibited three oxidation peaks. The initial peak at the minimal potential resulted from the oxidation of catechol and galloyl on the flavonoid B-ring, succeeded by the oxidation of malvidin anthocyanin, and ultimately by the subsequent oxidation wave of flavonoid phenolic groups [51].

E. Ott et al. employed square-wave adsorptive stripping voltammetry (SWAdSV) for the detection, identification, and semi-quantification of fentanyl in confiscated drug

samples, utilizing a quick, uncomplicated, and sensitive method using SPCEs. The electrochemical oxidation of fentanyl produced two anodic peaks: peak I at 0.75 V and peak II at 0.88 V, measured against an Ag/AgCl pseudo-reference electrode. Voltammetric measuring parameters were optimized for fentanyl standards between 0.076 and 6.9 $\mu\text{g mL}^{-1}$, resulting in a detection limit of 0.037 $\mu\text{g mL}^{-1}$ [52]. The ecstasy analog 3,4-methylenedioxyethylamphetamine (MDEA) was electrochemically screened for in forensic samples by Novais et al. using an SPCE and SWV. For MDEA screening, the best results were obtained using SWV (a: 40 mV, f: 30 Hz, Estep: 4 mV) and a Britton Robinson buffer solution of 0.04 mol L⁻¹ at pH 3.0, ensuring maximum sensitivity and selectivity. Strong sensitivity (0.569 $\mu\text{A}/\mu\text{mol L}^{-1}$), low theoretical limit of detection (0.03 $\mu\text{mol L}^{-1}$), robust repeatability, and a wide linear range (2.5 to 30.0 $\mu\text{mol L}^{-1}$, $R^2 > 0.99$) are all characteristics of this technique [53].

3.4. Electrochemical Impedance Spectroscopy (EIS)

EIS is an information-rich method that provides valuable insight into SPCE behavior, especially the effects of surface modification. In EIS, a small (5–10 mV) sinusoidal potential excitation about a set fixed potential is applied to the electrochemical system, and the time-varying current response is recorded. The frequency of the potential excitation is stepped through a series of values over a wide range of frequency from mHz to MHz. The current response will have a phase shift, and one of the ways that the data can be represented is a Nyquist plot with the real part of the impedance along the x -axis and the imaginary part of the impedance along the y -axis, and with each data point representing the result at a specific frequency. The data are then fit to an equivalent circuit model, from which several parameters are extracted, including the Warburg impedance, double-layer capacitance, and charge transfer resistance. The charge transfer resistance (R_{ct}) is a good diagnostic of the efficiency of electron transfer at the electrode surface and how this responds to surface modification. EIS can be compared to cyclic voltammetry and other methods that specifically look at nonlinear behavior [54]. It can assess the electrical double-layer capacitance (C_{dl}) that is present at the interface of the electrode and electrolyte solution [55,56].

EIS Nyquist plot of the SPCE substrate exhibits a capacitive loop at high frequencies in the absence of surface modification, which is connected to the R_{ct} and C_{dl} . At low frequencies, the semi-infinite diffusion type Warburg impedance (Z_W) of electroactive species in the electrolyte surrounding the electrode surface is associated with a straight line with a slope of around 45°. The SPCE has R_{ct} and C_{dl} values of 17,300 Ω and 5.0 $\mu\text{F cm}^{-2}$, respectively. The bare SPCE's high charge transfer resistance points to a Faradaic process limitation. For a free electroactive carbon surface, the SPCE electric double-layer capacitance is normal. Similar electrochemical impedance responses are shown by unmodified SPCEs in $\text{Fe}(\text{CN})_6^{3-/4-}$ with 0.1 M KCl and PBS electrolyte. The EIS responses of the modified SPCEs differ considerably from those of the unmodified ones [32,57]. A key goal of the modification of SPCE surfaces is to improve the efficiency of electron transfer, and this is reflected in a reduction in the value of R_{ct} . However, other modifications, such as the formation of polymer layers and protective coatings, can increase R_{ct} . The impact of preventing electron transfer on the electrode surface, which results in a significant increase in R_{ct} , is usually indicated by enlargement of the semicircular part of the Nyquist plots. In terms of quantification, EIS proves to be more informative than the CV approach [56,58,59].

Ward et al. aimed to investigate a cost-effective screen-printed electrode as a sensor for detecting *S. aureus* by EIS. *Staphylococcus aureus* was incubated in chambers with electrodes, and the findings were analyzed using an innovative normalization method. The results indicated that *S. aureus* can be detected in LB media during a 30 min incubation of a 1%

growth culture, as well as immediate cell concentration-dependent alterations in 0.9% NaCl. These data indicated that several electrochemical mechanisms alter the impedance due to the presence of *S. aureus*, including adsorption to the electrode surface and bacterial metabolism during growth. The research indicates that this detection method will be beneficial in several clinical situations when *S. aureus* causes infections that are challenging to manage [60].

Choi et al. used EIS to investigate changes after modifications of the electrochemically polymerized MIP on the SPCE, revealing surface impedimetric characteristics and identifying subtle variations at the MIP sensor surfaces. All EIS investigations employed a fixed 0.2 V bias potential. They performed initial EIS measurements on uncoated and MIP-coated SPCEs in the identical redox probe solution prior to and after cytokine IL-1 β extraction. A thin poly(o-PD) coating was applied to the SPCE via a 1-cycle CV method, leading to an expanded semicircle attributable to a less conductive polymer matrix. The MIP film produced on the SPCE/poly(o-PD) surface through electropolymerization with the C2R monomer and IL-1 β elevated R_{ct} to 17,440 Ω , attributed to the insulating IL-1 β imprint on the P(C2R) film, which obstructed electron transfer [61]. Using CV and EIS, Randviir et al. created an electroanalytical sensing platform comprising screen-printed carbon nanotube electrodes (SPEs) to identify capsaicin in artificial solutions and from sauces and chillies. Depending on the analyte concentration, several capsaicin electroanalytical detection methods were used. For large concentrations, when the waves mixed and moved out of the potential window, EIS was more suited than CV. The technique-specific preferences for both single-walled and multi-walled screen-printed carbon nanotube electrodes were also discovered. Based on analytical findings, single-walled (SW-SPE) was recommended for low-capsaicin concentrations, while multi-walled (MW-SPE) was preferable for high-capsaicin concentrations [62].

3.5. Linear Sweep Voltammetry

Linear Sweep Voltammetry (LSV) is a pivotal and significant technique in electroanalytical chemistry whereby the current at a WE is recorded as the potential between the WE and an RE is linearly varied over time at a fixed rate. The Randles–Sevcik (RS) theory primarily relies on the assumption of diffusion restriction of the active species in a neutral liquid electrolyte and rapid reactions at the working electrode. The RS theory applied to measurements as a function of scan rate using a redox probe of known diffusion coefficient can be used to estimate the electroactive surface area. Determination of the electroactive surface area can be important in assessing the effect of surface modification on an SPCE. In the instance of LSV, a constant potential range is used, akin to the potential step measurements [63,64]. This method is useful for studying reaction processes and determining a number of kinetic and thermodynamic characteristics [65].

Alharthi et al. reported making (ϵ -MnO₂/S@g-C₃N₄) using hydrothermal methods to make a dopamine (DA) sensor. The ϵ -MnO₂/S@g-C₃N₄ hybrid was used as an electrocatalyst to change the active area of the SPCE, which achieved a sensitivity of 1.53 μ A μ M⁻¹ cm⁻², and the LOD was 1.12 μ M, which is very good. DA detection that was steady, specific, and repeatable was shown by the ϵ -MnO₂/S@g-C₃N₄-modified SPCE. The modified SPCE also showed that it could detect dopamine in a steady, reliable, and specific way using the LSV [66]. Henawee et al. described a simple, low-cost way to make a carbon nanotube bulk-modified stencil-printed electrode (CNTs-SP) for measuring vortioxetine hydrobromide (VOR) in medicine formulas and biological fluids using LSV. The method is sensitive because VOR can stick to the surfaces in a controlled way and interacts well with the CNTs. The best settings for the experiment made the method linear from 3×10^{-8} M to 5×10^{-6} M in concentration, with a detection limit of 1×10^{-8} M in water and living fluids.

The process is easy, quick, and hard for the green science [67]. B. Shoub et al. employed a SPCE with AuNPs/ionophore to develop a sensitive and selective sensor for lead ions, utilizing linear sweep anodic stripping voltammetry (LSASV). They systematically varied electrochemical parameters, including supporting electrolyte, pH, deposition potential, deposition duration, and scan rate, to investigate their effects on the sensor's sensitivity for detecting Pb^{2+} [68].

3.6. Chronoamperometry

Chronoamperometry (CA) is an electrochemical technique in which electrode potentials are stepped from an inactive state (E1), where no electron-transfer reaction takes place, to an active state (E2) beyond the redox species' formal potential, where the rate of electron transfer is no longer the limiting factor for the electrode reaction [29]. It is used for deposition at a constant potential over a certain time [69]. It is also used for monitoring currents produced by an electrochemical reaction of the analyte on the SPCE surface.

CA was used with an SPCE modified by graphite nanoparticles and the enzyme D-fructose dehydrogenase (FDH) for the detection of fructose. Calibration was performed using fructose solutions (0.20 mM to 32.00 mM in water). McIlvaine buffer was used to prepare FDH solutions of 50 or 200 U mL^{-1} . SPCEs were used to measure the enzyme activity by depositing 20 μL of FDH solution, then 10 μL of 12 mM ferricyanide, and finally 10 μL of a standard fructose solution. The voltage was stepped from 0 V to +0.3 V versus Ag/AgCl after waiting for 180 s and stirring for 20 s. Twenty seconds after the voltage was applied, currents were recorded and used to make calibration plots, and a linear range from 0.1 to 1.0 mM was found, making the method promising for determining fructose in commercial fruit juices [70].

Phasuksom et al. developed a chronoamperometric enzymatic glucose sensor on SPCEs. The electroactive surface area and current responsiveness were increased by coating with doped-polyindole (dPIn) and MWCNTs. Chitosan and glucose oxidase (CHI-GOx) were immobilized on the electrode. 3-Aminopropyl triethoxysilane (APTES) connected CHI-GOx and dPIn. The glucose sensor's current response increased in a power law-like manner with glucose concentration. Glucose was detected in blood and urine samples. After four weeks of storage, the enzymatic glucose sensors showed exceptional stability and selectivity despite diverse interferences. The sensor also monitored glucose continuously or step-by-step. The preparation method was straightforward and suitable for mass production. This glucose sensor uses a three-electrode SPCE cell and is straightforward to operate. It might become a diabetes glucose monitoring prototype [71].

Jo et al. used chronoamperometry to develop a sandwich aptamer-based SPCE electrodeposited with AuNPs and an electropolymerized conductive polymer for detecting cardiac troponin I (cTnI), which could serve as a marker for an acute myocardial infarction (AMI). The amount of cTnI was measured using amperometric readings from the reaction between hydrazine and H_2O_2 . The aptasensor worked very well for analysis, both in buffer and serum-added solution. It had a dynamic range of 1–100 pM (0.024–2.4 ng mL^{-1}) and a LOD of 1.0 pM (24 pg mL^{-1}) [72].

4. Use of SPCEs in Flow Injection Systems

Numerous studies have sought to improve the efficiency, repeatability, sensitivity, selectivity, and ease of handling of electrochemical methods by combining them with flow or batch injection analytical techniques. These approaches include voltammetry and amperometry. There is a decrease in both waste and instrument costs because of this. For them to function, a small quantity of samples is introduced into a carrier stream. Either the sample may be processed before reaching the electrode, or it can be transported without

undergoing any chemical reactions. Flow injection analysis is the most used technique for injection analysis. The simplicity with which it may be used to set up tests is one reason why FIA has grown in popularity since its 1974 debut. It is believed that the next generation of FIA will be sequential injection analysis (SIA), which was published in 1990. For jobs involving complex chemical processes, SIA's foundational multiple-port valve makes accurate sampling and chemical handling a breeze. In addition, the flow pipe configuration does not need to be changed to connect it to other devices. There are many types of injectable analyses; the simplest is batch injection analysis (BIA), which has been around since 1991. For routine analyses, its primary instrument, an automated pipette, may be invaluable. The combination of injection analysis methodologies and SPEs is continuously being researched and has been the subject of several scientific articles. The acronyms FIA, SIA, BIA, and SPEs are all the focus of separate review articles. As far as we are aware, there has been little analysis so far of the combination of all flow injection techniques and SPEs, with an emphasis on the developments from the past few years [73,74].

Marzouk et al. created three unique cells for flow-injection, thin-layer, and batch electrochemical assessments utilizing screen-printed electrode chips (SPECs). All cells had an acrylic foundation and a clear acrylic cover, as shown in Figure 3. The architecture of each cell foundation included a chamber for the SPEC, while the transparent acrylic cover defined the cell form and function. The presented cells have several advantages, including easy SPEC connection to any potentiostat without cables, complete SPEC containment, compatibility with various commercial SPECs, and excellent SPEC sealing. The flow cell allows for easy modification of dead volume and visual observation of SPEs and their surroundings. A specialized thin-layer cell with near-ideal steady-state voltammetry employing SPECs is shown for the first time. The universal batch cell (UBC) is versatile and ideal for batch applications in 25 μL to 40 mL sample sizes, with optional regulated temperature and environment. Additionally, a new method for stirred-solution chronoamperometry and hydrodynamic voltammetry employing SPECs with improved signal-to-noise ratios is shown using the UBC [75].

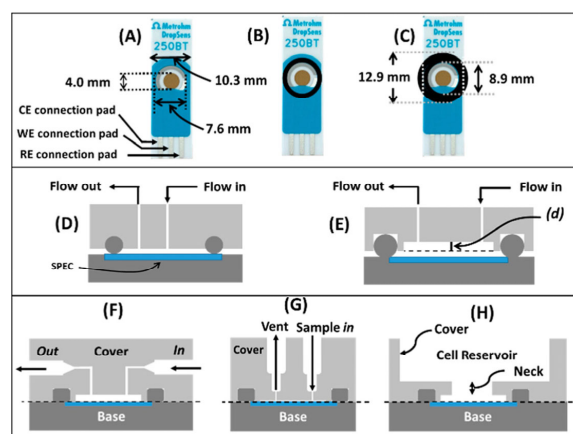


Figure 3. Common three-electrode SPEC layout and size (A). The current general cell design and the O-ring sizes utilized in commercial design are shown in (B,C), with matching cross-section layouts illustrated in (D,E), respectively. The O-ring represented in (E) is larger than the one in (D). A machined groove in (E) denoted as (d) is used to control the dead volume. From (F–H), the cross-sectional designs of the completed FC, TLC, and UBC are shown, respectively. Reproduced from ref. [75], with permission from the American Chemical Society, copyright 2021.

Upan et al. were able to successfully create a simple screen-printed electrode that can be used in an electrochemical sensor to measure hydroquinone using a flow-injection

amplifier system. It is easy to see that SPCE-CNT is sensitive and reliable because it transfers electrons well. The enzyme column is simple to make and works well to speed up the oxidation of hydroquinone. This method has a lot of benefits, such as it is inexpensive, takes only a short time to analyze, and uses few chemicals and samples. The sensor produced good results in terms of accuracy, sensitivity, wide linear range, and low detection limit, as shown by the results [76].

Shih et al. investigated how the antibacterial and antifungal zinc pyrithione (ZPT) is used in shampoos to remove dandruff at concentrations of up to 1%. Oral intake is bad for both people and animals in several ways. A throwaway CoPc/SPE screen-printed carbon electrode and FIA were used to enable easy and specific detection of ZPT in commercial hair care items. At 0.3 V and 0.1 M KOH in a solution with Ag/AgCl, the CoPc/SPE showed a straight-line calibration plot (6–576 M) with sensitivity and detection limits of $1.65 \text{ nA } \mu\text{M}^{-1}$ and 0.9 mM (i.e., 1.42 pg in a 5 μL sample loop) under the best FIA conditions. This method is easy to use, specific, and inexpensive, so it can be used for regular ZPT research in hair care items [77]. Sha et al. investigated the electrooxidative polymerization of azure B on SPCE in a neutral phosphate buffer, which demonstrated superior electrocatalytic activity and stability for the oxidation of dihydronicotinamide adenine dinucleotide (NADH) in phosphate buffer (pH 6.9), exhibiting an overpotential exceeding 400 mV lower than that of the unmodified electrodes. The modified SPCE showed potential as an amperometric detector for FIA of NADH, generally exhibiting a dynamic range of 0.5 mM to 100 mM [78].

5. Electrochemical Sensors Based on Unmodified SPCE

Electrochemistry has paid a lot of attention to the creation of new electrodes with different modifications up to this point. They are expensive, hard to work with, and not good for the environment, among other things. Hence, the first electrochemical sensor for measuring palladium ions (Pd^{2+}) using an unmodified screen-printed carbon electrode has been created. Using CV, the operational conditions of the unmodified SPCE were optimized before the determination of Pd^{2+} ions, and the electro-analytical behavior was good for the determination of Pd^{2+} ions. By using differential pulse voltammetry to measure the concentration of Pd^{2+} ions, it was found that the unaltered electrode had a detection limit of $1.32 \text{ } \mu\text{M}$ and a linear range from 3 to $133.35 \text{ } \mu\text{M}$. The new sensor was also successfully used to find small amounts of Pd^{2+} ions in water samples that had been spiked. Another benefit of this type of electrode is that it is easy to use, can be thrown away, and is inexpensive for electrochemical devices [79].

The disparities in LOD between the unmodified SPCEs are substantial yet anticipated. SPCEs offer significant advantages for field analysis because of their compact dimensions and functionality, which frequently constitutes a favorable compromise. Furthermore, although marketed for single use, the same SPCE can be reused for repeated assessments without a substantial decline in measurement sensitivity. This is particularly pertinent given the examination of an extract comprising 50% organic solvent (ethanol), which appeared to preserve the integrity of the ink on the ceramic substrate. Goncalves et al. obtained a linear association between the anodic peak current and the concentration of vitamin D3, which was established within the range of 59.4 to $1651 \text{ } \mu\text{mol L}^{-1}$ for the SPCE under optimal circumstances. The LOD was $19.4 \text{ } \mu\text{mol L}^{-1}$ using SWV, demonstrating the efficacy and use of bare, unmodified SPCEs for the analysis of Vitamin D3, eliminating the necessity for more sophisticated solid electrodes or surface modifications [80]. SPCEs are increasingly recognized as electrochemical sensors in clinical and environmental domains due to their reproducibility and scalability. Moreover, the constituents of SPCEs, including carbon inks and polymeric binders, are notably appealing due to their cost-effectiveness,

little background currents, and extensive potential windows, which demonstrate varied electroanalytical properties [81].

Das et al. characterized the bare screen-printed carbon sensor strips in terms of their material composition before detecting T4. They obtained LOD of 3 nM by using DPV and CA. The cyclic voltammogram of the potassium ferricyanide redox pair on SPCE demonstrates that the difference between the anodic and cathodic peak potentials is less than that of the chemically modified carbon paste electrode (CPE). Furthermore, it has been demonstrated that the electroanalytical performance of bare SPCE surpasses that of standard CPE. This is likely attributable to the composition and microscopic structure of the specific carbon-based components and binder employed. The SEM picture of the SPCE surface reveals flake-like graphite particles coated with a polymeric binder. The energy-dispersive X-ray analysis (EDX) of the uncoated electrode indicated 93 atomic weight percent carbon and 5 atomic weight percent chlorine, respectively. The mean roughness value was recorded as 2.3 mm [82].

There are limitations to SPEs, even though they are important candidates for fast diagnosis. For example, the method's selectivity can be compromised due to cross-reactions with other non-target compounds. It seems that the reference electrode of commercially available SPEs has a tiny layer of silver. Therefore, it usually starts to deteriorate after a couple of CV and impedance measurement cycles. Even when stored in a refrigerator, their stability is low; therefore, extreme care is required after functionalization. That is why it is important to think about the conservation of SPE-based biosensors alongside their performance. Some researchers have developed a hybrid microfluidic sensor that can detect tiny amounts of cocaine in both water and bodily fluids by combining the ELISA concept with SPEs. Combining molecular approaches for selective sequence amplification with functionalized screen-printed electrodes to detect the amplified product can also lead to new and improved diagnostic methods [83]. There is an ongoing need in the analytical area to provide platforms and methodologies that are sensitive, inexpensive, and user-friendly. Affordable printed electrodes, which may be readily downsized and obtained with homemade equipment when needed, offer a viable alternative. With its low background current, large potential windows of use, and resistance to a wide range of solvents, carbon ink is an ideal platform to be changed with many kinds of materials, such as nanomaterials, organic macromolecules, or polymers. But the (nano)modified surface causes an electrocatalytic behavior that is totally modifier-dependent [84].

Table 1 shows SPCE modifications with various materials, along with the detection techniques used in real-world samples and their LOD and linear ranges.

Electrode structure abbreviations: MIP: molecularly imprinted polymer; NPs: nanoparticles; Ab-HAS: antibody for human serum albumin; AuNCs: gold nanocrystals; MWC-NTs: multi-wall carbon nanotubes; Anti-EE2: antibody for EE2; SNs: silica nanoparticles; r-GO: reduced graphene oxide; Cys: cysteine; 4-CP: 4-carboxyphenyl diazonium salt; pp-AN: polymerized acrylonitrile; PANI-CHT: polyaniline–chitosan composite; PAPBA: poly-3-aminophenylboronic acid; H-FeMoSe₂: hydrothermally prepared Fe doped MoSe₂; AgNPs-GO: silver nanoparticles—graphene oxide; LDH: lactate dehydrogenase; b-CD: β-cyclodextrin; EB-p-TBA: Evans blue + poly(2,2':5',5''-terthiophene-3'-p-benzoic acid); HPC: eteroatoms (N and S) doped porous carbon (HPC); MIP-P-o-PD: poly(o-phenylenediamine)-based molecularly imprinted polymer; APTES: 3-aminopropyltrimethoxysilane; Tyr: tyrosinase; NG: nitrogen doped graphene; PVP: polyvinylpyrrolidone; PANI: polyaniline; OE: orange peel extract; LE: lemon peel extract; poly(L-cys): poly-L-cysteine; SPrGOE: Screen-printed reduced graphene oxide electrode; OAP: o-aminophenol; HMA: hexamethylthylamine; cfAuNP: Cauliflower-shaped gold nanoparticles; SPpTE: screen-printed platinum electrode.

Table 1. Various analytes electrochemically detected by the modification of SPCEs, and the essential experimental parameters of the limit of detection and linear range.

Electrode Structure	Real World Sample Studied	Analyte	Detection Method	Limit of Detection	Linear Range	Reference
MIP/Graphene/SPCE	Human serum and tablet	STR	DPV	1.99×10^{-9} M	5.0×10^{-9} to 7.5×10^{-7} M	[85]
Recombinant SARS-CoV-2 spike protein antigen/Ni(OH) ₂ NPs/SPCE	Human serum	SARS-CoV-2-specific viral antibodies.	DPV	0.3 fg mL^{-1}	1 fg mL^{-1} to $1 \text{ } \mu\text{g mL}^{-1}$	[8]
Ab-HSA/AuNCs/Polyaniline/SPCE	-	HSA	EIS	$3 \text{ } \mu\text{g mL}^{-1}$	$3\text{--}300 \text{ } \mu\text{g mL}^{-1}$	[6]
Nafion/MWCNT-SPCEs	Human urine and serum	ETB	SWV	$8.4 \times 10^{-4} \text{ mg } \mu\text{L}^{-1}$		[86]
Anti-EE2/Paper microzones + SNs/r-GO/SPCE	River water	EE2	SWV	0.1 ng L^{-1}	$0.5\text{--}120 \text{ ng L}^{-1}$	[87]
Cyst/4-CP/SPCE	Water samples	Cd (II)and Pb(II)	SWASV	0.882 nM Cd (II) and 0.65 nM Pb (II)	$0.01 \text{ } \mu\text{M}$ to $0.7 \text{ } \mu\text{M}$	[4]
pp-AN/SPCE sensor	River, ground, and wastewater, synthetic urine, and human serum	Bupropion	SCV	$0.21 \text{ } \mu\text{mol L}^{-1}$	$0.63\text{--}10.0$ and $10.0\text{--}50.0 \text{ } \mu\text{mol L}^{-1}$	[88]
PANI-CHT/SPCE	Industrial, rural, and residential water samples	PFOA	DPV	1.08 ppb	$5\text{--}150 \text{ ppb}$	[89]
PAPBA/AuNPs/SPCE	Plasma sample	MI	CV	1.0 nM	500 nM to $60 \text{ } \mu\text{M}$	[90]
H-FeMoSe ₂ /SPCE	Paramedical tablet	MES	DPV	0.8 nM	$0.004\text{--}57$, $63.57\text{--}145.59 \text{ mM}$	[42]
Pd-CNT/SPCE	Disinfectant, hair colorant, and milk samples	H ₂ O ₂	FI-Amp	$20 \text{ } \mu\text{M}$	$0.1\text{--}1.0 \text{ mM}$	[5]
AgNPs-GO/SPCE	Human serum	PSA	DPV	0.27 ng mL^{-1}	$0.75\text{--}100.0 \text{ ng mL}^{-1}$	[91]
Apt/AuNR/SPCE	Human urine and plasma	BCM-7	DPV	334 amol L^{-1}	1 fmol L^{-1} to 25 nmol L^{-1}	[13]

Table 1. Cont.

Electrode Structure	Real World Sample Studied	Analyte	Detection Method	Limit of Detection	Linear Range	Reference
LDH/SPCE	Human sweat	Lactate	EIS	0.1 mM	0.1–100 mM	[92]
β -CD/MWCNTs/SPCE	Human serum	Cholesterol	DPV	0.5 nM	1 nM to 3 M	[81]
EB-p-TBA/HPC/SPCE	Human blood plasma	NTs	CA	0.034 nM	0.05–130 nM	[93]
MIP-P- <i>o</i> -PD/APTES/Au/O ₂ /SPCE	Human serum	IL-6	DPV	1.74 pg mL ^{−1}	2 to 400 pg mL ^{−1}	[94]
Au-SPCE Cu/Au-SPCE	Cartridge, shooting, and explosive samples	Pb, Sb, and Zn Nitrate, Nitrite	ASV LSV	51, 29, 67 mM 130, 120 mM	100–700 μ g L ^{−1} 0–0.6 mM	[95]
Tyr/GA/ZnO NPs/SPCE	River, well, and tap water	Chlortoluron	CA	0.02 μ M	1–100 nM	[96]
NG/PVP/AuNPs/SPCE	Fruit and vegetable samples	Hydrazine	SWV	0.07 μ M	2–300 μ M	[97]
ZnO NPs/MWCNTs/LSPCE		Glucose	CV	0.43 mM	1–100 mM	[36]
PANI@BiVO ₄ nanoflakes/SPCE	Human serum	As ³⁺ ions	DPASV	0.0072 ppb	0.01 to 300 ppb	[98]
MWCNTs-CS/SPCE	Plasma	Indole	DPV	0.5 μ g L ^{−1}	5–100 μ g L ^{−1}	[99]
MIP/Ag-Au NPs/SPCE	Sweat	Lactate	Amperometry	0.003 μ M	1–220 μ M	[100]
LE/ZnO NPs/Cu ₂ O NPs/PANI/SPCE OE/ZnO NPs/Cu ₂ O NPs/PANI/SPCE	-	Cd ²⁺ and Hg ²⁺ ions	SWV	3.04, 1.08 ppb 5.08, 2.72 ppb	2.2–12 mM, and 0.17–1.5 mM for Cd ²⁺ 2.95–11.8 mM and 0.12–1.2 mM for Hg ²⁺	[26]
AuNPs/SPCE	Whole blood	HbA1c	DPV	8.34 pg mL ^{−1}	1 to 104 pg mL ^{−1}	[101]
poly(L-Cys)@SPrGOE	Human serum	Olanzapine	SWV	0.91 nM	10–1000 and 1500–5000 nM	[102]
Apt/HMA/SPCE	Beer samples	OTA	DPV	0.1 mg L ^{−1}	0.12–8.5 mg L ^{−1}	[103]
cfAuNPs/SPCE	Human serum and honey	hIgG H ₂ O ₂	DPV CA	0.11 ng mL ^{−1} 0.66 ng mL ^{−1}	0.11–50 ng mL ^{−1} 0.7–70 ng mL ^{−1}	[9]
Au/SPCEs Au/SPPtEs	-	CAP	CV DPV	0.2 mM	0.25–50 mM	[104]

Analytes: STR: sertraline; HSA: human serum albumin; ETB: ethambutol; EE2: ethinylestradiol; PFOA: perfluorooctanoic acid; MI: myo-inositol; MES: mesalamine; H_2O_2 : hydrogen peroxide; PSA: prostate specific antigen; BCM-7: β -casomorphin; NTs: neurotransmitters; IL-6: interleukin-6; HbA1c: glycated hemoglobin; OTA: Ochratoxin; hIgG: human IgG; CAP: chloramphenicol.

Methods: CV—cyclic voltammetry; CA—chronoamperometry; DPV—differential pulse voltammetry; EIS—electrochemical impedance spectroscopy; SWV—square wave voltammetry; SWASV—square wave anodic stripping voltammetry; DPASV differential pulse anodic stripping voltammetry; ASV—anodic stripping voltammetry; LSV—linear stripping voltammetry; EC—electrochromatography; FI-AMP—flow injection amperometry; SCV—staircase voltammetry.

6. Surface Modification of SPCE for Use in Electrochemical Sensors

SPCEs are inexpensive and provide a wide electrochemical potential window, which are two characteristics that are desirable in chemically modified sensors. In comparison to other chemically modified electrodes, such as nanocomposite modified GCE or zirconia cube-modified gold electrodes, SPCE is highly selective because it is less reactive and has a weak electrocatalytic reaction to analytes because of the graphitic defects [98]. Improvement of SPCE electrochemistry can be achieved via pretreatment, electrochemical activation, or surface modification utilizing nanomaterials and polymers, and plasma treatment, as shown in Figure 4, which are among the few straightforward and efficient methods for surface modification of SPCE. Pretreatments encompass plasma treatment, immersion in organic solvents, exposure to UV/ozone, and electrochemical cycling in a range of solvents. Surface modification with materials or molecules capable of rapid electron transfer or serving as redox mediators can improve the sensitivity by increasing the efficiency of electron transfer, and this is often seen as a reduction in R_{ct} if the electrode is characterized using EIS. Surface modification can also involve immobilizing receptors for specific analytes, such as supramolecular hosts, antibodies, or aptamers. Additionally, an enzyme that acts specifically on the analyte may be placed on the SPCE surface. Many studies use simple drop-casting, while others carry out covalent conjugation to the surface through some linking molecules or polymer functional groups. Molecularly imprinted polymer (MIP) films on SPCE have also been reported, and while proving specificity, these generally increase the R_{ct} value.

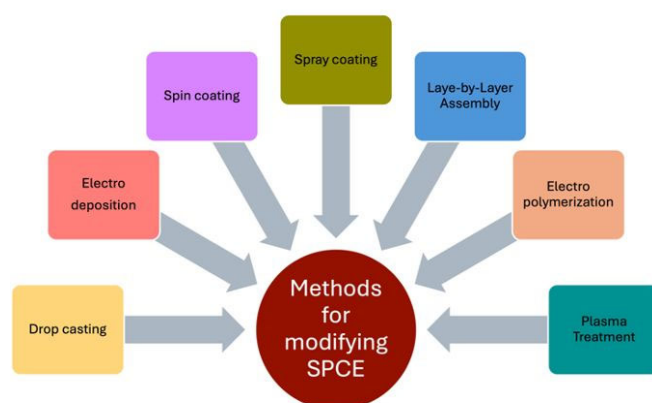


Figure 4. Methods for modifying SPCE.

6.1. Modification Methods for SPCE

The modification of SPCEs can be achieved through several ways, like electrodeposition [105,106], layer-by-layer assembly [107–109], electro polymerization [110–112], plasma treatment [113,114], spin coating [115,116], spray coating [117,118], and drop-

casting [119–121], as shown in Figure 4, to improve the electrochemical selectivity and sensitivity, and their performances are described in Table 2. Nanomaterial modification through drop-casting is a prevalent technique employed to regulate the electrochemically active area of the electrode surface and the subsequent electrochemical behavior. Common nanomaterials consist of metallic nanoparticles and carbon-based nanoparticles (carbon nanotubes, carbon black, and graphene or graphene oxide) [122–124].

Table 2. Summary of methods for modifying SPCE and their performance.

Modification Method	Performance	Ref.
Drop-casting	Used manually for small areas; produces a non-uniform layer and is hard to reproduce. It is quite easy to modify any electrode with it, and it produces transparent, flexible, and conductive films.	[119–121]
Electrodeposition	Performed in aqueous solutions under mild conditions for modification of metals, alloys, and self-controlled and high-performance electrodes.	[105,106]
Electro polymerization	Uses conducting monomers to coat electrodes, controls the polymer thickness, and prevents electrode fouling.	[110–112]
Spin Coating	Used in microfabrication to form a desired uniform film/layer on a flat surface by using a spin coater.	[115,116]
Spray coating	Used to coat on a large scale with high-speed application to produce a non-uniform film through the nozzle of a sprayer.	[117,118]
Layer-by-layer assembly	Simple, robust, cost-effective, and versatile method to coat and deposit controlled uniform layers on substrates by using an oppositely charged material layer-wise.	[107–109]
Plasma Treatment	Uses ionization processes to modify and catalytically modify the surface without damaging it.	[113,114]

6.2. Types of Modifications

Detection with just SPCE could be challenging as it lacks innate selectivity and sufficient activity, necessitating surface modification of the electrodes [101]. Types of modification depicted in Figure 5, such as nanoparticles, other nanomaterials, polymers, MIP, and composites/hybrid materials, can increase the electron transfer rate and electrode surface area in comparison to conventional materials [99]. Table 3 shows an overall comparison of different types of modification.

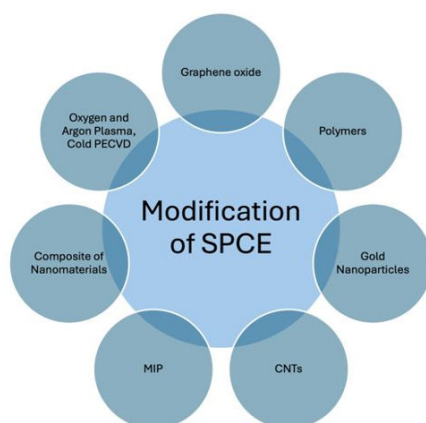


Figure 5. Types of surface modification of SPCEs.

Table 3. Comparison of different types of surface modification of SPCEs.

Modification Type	Selectivity	Sensitivity	Fabrication Complexity	Scalability	Stability
Gold-based nanomaterials	Extremely High	Very High	Low to High	Moderate	High
Carbon-based nanomaterials	Low	Very High	Moderate	Very High	Good
Polymers	Low, but can be engineered	High	Low to Moderate	Low to High	High
MIP	High	High	Extremely complex	Very Low	Moderate to High
Plasma treatment	Low	High	Low	High	High
Biological recognition elements (aptamers, antibodies, enzymes)	High	High	High	High	Low

6.2.1. Plasma Modification

Plasma technology is well-known for improving coating adhesion by molecularly altering polymer surfaces chemically and morphologically. Compared to other surface modification technologies, plasma treatment has several benefits, including low reagent consumption, environmental friendliness, material versatility, the capacity to generate carboxyl groups, and treat numerous electrodes in a brief period (5 s). Additionally, it has the capacity to eliminate grime and binders from the electrode surface and uses an operating temperature that is close to ambient [92,124].

Cold Atmospheric Plasma Modification

With cold atmospheric plasma (CAP) technology, plasma treatment can be performed under atmospheric conditions, significantly reducing the initial capital investment. Because of its straightforward design, lack of toxicity, and lack of environmental impact, CAP has proven to be far more effective than conventional surface treatment methods for tasks such as surface activation, coating deposition, and surface cleaning. In this work, we present the first report on using CAP to show that a surface treatment can increase the stability of sensor response over time by lowering drift. In addition to removing the paste binder and revealing the SPCE surface's more pure graphitic composition, the CAP treatment also generates the necessary functional groups, including hydroxyl, carbonyl, and carboxyl ones. For solid-state ISE-based potentiometric sensors to work reliably over time, these functional groups are essential for forming a strong interfacial connection between SPCE and ISM, which in turn reduces the water layer at the interface [10].

Oxygen Plasma Modification

Oxygen plasma is used to decontaminate surfaces prior to bonding, introduce oxy-functionalities to the surface, and create nanoscale roughness through surface etching. The primary dynamic species in plasma that interacts with the outer layer of fibers may lead to the bonding, abstraction of electrons, and enhancement of oxy/nitro-functionalities on the polymeric surface. Nevertheless, the reactive organic monomeric plasma results in plasma polymerization, grafting, and deposition onto the surface [125]. A cold reactive oxygen plasma process greatly enhances the transfer of electrons and creates oxygenated and carboxyl functional groups on the surface of SPCEs. These groups likely make the 3D-printed electrode more electrochemically effective. This protocol works better for elec-

trochemistry than any other way described in the literature that uses chemical, biological, or electrochemical treatments. It is also faster (2 min), better for the environment (no chemicals used), and has fewer steps [124,126].

As a result, the formation of carboxyl groups on the electrode surface, alterations in surface charge, enhanced capacitance, and improved hydrophilicity were noted. The alterations can be ascribed to the formation of carboxyl groups on the electrode surface, indicating that O₂-plasma treatment is a straightforward and efficient approach for surface modification. The O₂-plasma-treated electrode exhibited greater sensitivity for immunoglobulin A (IgA) compared to the untreated electrode, as the covalently attached antibody mitigated nonspecific adsorption due to the previously described surface modifications [124]. Chang et al. utilized oxygen plasma to selectively etch SPCEs. The coefficient of variance (CV) for inter-electrode reproducibility decreased from 21.6 to 4.6. Analysis of the surface using color-level-indexing histogram techniques, scanning electron microscopy (SEM), and resistance measurements indicated that the reproducibility between electrodes was associated with the thorough removal of the resin binder from the surface of the SPCE. This color level index analysis was utilized to differentiate the quality of the electrode. This technique demonstrates significant potential for implementation in online quality control of the SPCE plasma-treatment process when combined with appropriate image processing software [127].

Prasad et al. studied radio-frequency oxygen plasma treatments at a pressure of 50 Torr and an exposure of 100 W plasma for 30 s, and the edge plane sites on SPCEs for the simultaneous determination of dopamine, uric acid, and ascorbic acid. Electrochemically preanodized and oxygen plasma-treated SPCEs were utilized to partially differentiate between these two effects. Raman and XPS investigations confirm that varying treatments can indeed elicit distinct surface features. The electrocatalytic activity improves significantly due to the large enhancement of surface-bound carbon–oxygen functional groups and/or the formation of edge plane sites via surface reorientation. A potential mechanism was suggested to elucidate the voltammetric behavior. The peaks for dopamine, uric acid, and ascorbic acid were distinctly differentiated from one another at the electrochemically preanodized SPCE, allowing for simultaneous detection at neutral pH by this straightforward method [128].

Cold Plasma-Enhanced Chemical Vapor Deposition

A novel method for altering screen-printed carbon electrodes with plasma-deposited acrylonitrile (pp-AN) nanofilms uses cold plasma-enhanced chemical vapor deposition (PECVD), which is a highly promising cold plasma method for electrochemical applications, utilizing volatile organic or organometallic compounds as precursors. This technique facilitates the deposition of extremely thin films ($\ll 1 \mu\text{m}$) on nearly any support of any configuration while preserving its dimensions. Through meticulous selection of the precursor composition and refinement of the deposition process, the molecular architecture of the resultant films may be accurately regulated. Catalytic materials synthesized by cold plasma processes can be utilized in fuel cells, rechargeable batteries, solar cells, and water-splitting devices. The application of the PECVD process in the fabrication of voltammetric sensors is typically linked to the generation or alteration of functional materials on silicon or metallic substrates, subsequently utilized as working electrodes, and it is quick and easy. Using the PECVD method allows for the simultaneous preparation of numerous sensors, ensuring uniformity and mechanical endurance of nanofilms. Variable deposition conditions, such as plasma discharge power and deposition duration, allowed for precise control over film molecular structure, nanostructure, and thickness. Changing PECVD process settings can significantly alter the properties of the produced sensors. The research demonstrates that

modifying the surface of screen-printed carbon electrodes allows for the creation of novel sensors for field research and monitoring systems [88,126].

Argon Plasma Treatment

To activate a carbon electrode that has been screen-printed but has a partially obstructed surface because of the polymer binder, treatment with argon (Ar) plasma was shown to drastically alter both the morphological aspect and electrochemical reactivity. The results show that the power of the argon plasma greatly affected the plasma treatment's effect. In addition to its activating action, Ar plasma offers an intriguing method for pre-assembling microelectrodes [129].

6.2.2. Modification by Gold Nanoparticles

Gold particles are significant due to their extensive effective surface areas. The particles enhance functional density, promote electron transfer, improve the electrochemical signal of the device, and are recognized for their high compatibility and conductivity, and are extensively used in electrochemical sensors and biosensors [104,123]. Kanyong et al. used AuNP-modified screen-printed carbon electrodes, referred to as AuNP-SPCE arrays, which were analyzed using CV and EIS. The AuNP-SPCE arrays exhibit remarkable electrocatalytic activity for lead and copper. Two distinct and fully resolved anodic stripping peaks are observed at 20 mV for Pb (II) and at 370 mV for Cu (II), both referenced to Ag/AgCl. Square wave anodic stripping voltammetry was employed to concurrently assess Pb (II) and Cu (II) in their binary combinations in tap water. The linear working range for Pb (II) spans from $10 \mu\text{g L}^{-1}$ to $100 \mu\text{g L}^{-1}$, exhibiting a sensitivity of $5.94 \mu\text{A } \mu\text{g}^{-1} \text{ L cm}^{-2}$. The data for Cu (II) indicate a working range of $10 \mu\text{g L}^{-1}$ to $150 \mu\text{g L}^{-1}$, with a sensitivity of $3.52 \mu\text{A } \mu\text{g}^{-1} \text{ L cm}^{-2}$. The detection limits, determined by three times the baseline noise, are 2.1 ng L^{-1} and 1.4 ng L^{-1} , respectively. This array is notably appealing as Pb(II) and Cu(II) may be quantified at very low working potentials, rendering the approach quite selective, as it is not substantially affected by other electroactive species that necessitate greater reduction potentials [130].

Syafira et al. compared bare SPCEs, and the SPCE treated with a hydroxyapatite-gold nanocomposite demonstrated a superior current response of $[\text{Fe}(\text{CN})_6]^{3-/4-}$. The ideal experimental conditions were an RBD-S concentration of $1 \mu\text{g mL}^{-1}$, an RBD-S incubation duration of 20 min, and an IgG incubation period of 10 min. Additionally, RBD-S was successfully immobilized on SPCE/HA-Au electrodes. The resultant electrode must be maintained in a refrigerated container with a suitable humidity level to maintain good function for seven weeks. In summary, when compared to previous serological techniques, the SPCE/HA-Au/RBD-S immunosensor exhibits good specificity, selectivity, and stability for the quick and precise detection of IgG SARS-CoV-2, which is followed by the successful identification of IgG in human serum samples. Tiered antibody detection helps identify the body's immune system and reduces the risk of SARS-CoV-2 virus reinfection. This study demonstrates the effectiveness of vaccination against the SARS-CoV-2 virus, as well as the future application of an immunosensor created for COVID-19 serological diagnostics [131].

Zakkiyah et al. studied the addition of AuNPs to SPCEs successfully using both drop-casting (DC) and spray-coating (SC) methods to improve biosensor performance for finding SARS-CoV-2 RNA. When compared to the SC method, the DC method deposited more AuNPs on the electrode surface, which improved the efficiency of electron transfer and increased the peak current reaction. On the other hand, the SC method gave a more even distribution of AuNPs, even though it had a smaller peak current response. Electrochemical tests with DPV and EIS showed that both methods had better conductivity and lower resistance. The DC method was more sensitive ($\text{LoD} = 0.166 \mu\text{g mL}^{-1}$) than the SC method

(LOD = $0.694 \mu\text{g mL}^{-1}$). The DC method had a higher sensitivity and a lower detection limit, but the SC method made voltammograms that were cleaner and had less noise. Both methods showed high selectivity because non-target RNA hybridization did not produce a signal that could be seen. Overall, the DC method works better for tasks that need high sensitivity, while the SC method is better for ensuring that all nanoparticles are covered evenly. This study also shows that SPCE/AuNP-based biosensors could be useful in clinical investigations and lays the groundwork for more progress in nucleic acid detection technologies [132]. Wang et al. created an SPCE using in situ deposition modification of AuNPs and L-cysteine to find As(III) in water and tea in a way that is sensitive, quick, easy, and handy using linear sweep anodic stripping voltammetry (LSASV). L-cysteine self-assembled onto AuNPs and helped the accumulation of As(III), which improved the specificity and sensitivity of As(III). It was able to measure as little as 0.91 ppb ($\mu\text{g L}^{-1}$), had a linear range of 1 to $200 \mu\text{g L}^{-1}$, a 5.3% inter-assay coefficient of variation, and was very specific. The new method was used to find As(III) in tap water and tea samples and worked well, with a recovery rate of 93.8% to 105.4%. It was also confirmed by inductively coupled plasma mass spectrometry (ICP-MS). The new method is quick, easy, and accurate. It shows strong potential for finding As(III) in tap water and tea leaves, and it can be used to find other things as well [133].

6.2.3. Modification by Carbon-Based Nanomaterials

More effective biosensor platforms have recently emerged because of developments in nanotechnology. The biosensor applications have skyrocketed due to the breakthroughs in synthesizing several novel nanomaterials with controllable morphologies and unique physicochemical properties. The development of electrochemical biosensor platforms has made extensive use of carbon-based nanomaterials, including graphene (G), graphene oxide (GO), single-wall carbon nanotubes (SWCNTs), multi-wall carbon nanotubes (MWCNTs), and carbon nanofibers (CNF), as shown in Figure 6, which have been used to directly identify a wide range of targets, such as small molecules and microorganisms, and determine if they are harmful or not. Carbon nanoparticles have demonstrated several intriguing characteristics, including excellent electrical conductivity, mechanical strength, surface-to-volume ratio, and chemical stability. Because of their exceptional qualities, these materials were perfect for use in creating electrochemical biosensors [87,134,135].

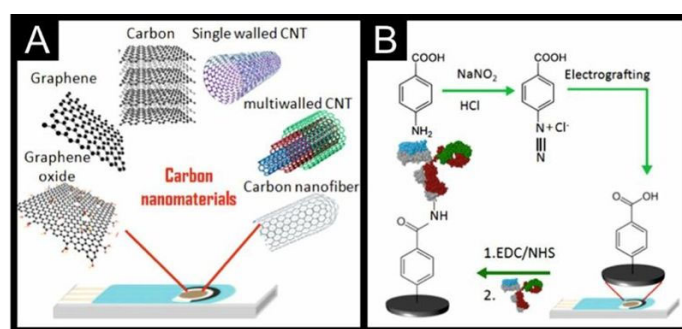


Figure 6. (A) Different carbon nanomaterial-modified screen-printed electrodes, (B) Functionalization of the electrodes via diazonium salt reduction and immunosensor fabrication. Reproduced from ref. [134], with permission from Elsevier, copyright 2018.

Graphene Oxide

Graphene is an excellent nanomaterial for enhancing the electrochemical performance of electrodes, particularly their sensitivity, because of its high levels of electrical conductivity, surface area, and physical/chemical stability [17,85,91]. The study found that a screen-printed carbon electrode tweaked with nanoplatelets of graphitic oxide (GO) made

the voltammetric peak separation and sensitivity of uric acid and ascorbic acid much better. We used electrochemical monitoring of uric acid and ascorbic acid to learn more about how oxygen functions and edge plane sites affect electrocatalysis at GO. We successfully used a microwave-assisted hydrothermal removal method to remove the functional groups from the GO surface that contain oxygen. The edge planes can be preserved on GO, and changing the microwave treatment temperature makes it easy to change the number of functional groups that contain oxygen. The ability to tell the difference between uric acid and ascorbic acid using this platform is due to their distinct ways of interacting with oxo-surface groups, especially the COOH group on GO, to form hydrogen bonds [136].

To track neurotransmitter (NT) levels in blood plasma, Seo et al. developed a new electrochemical microfluidic separation and sensing (EMSS) device. Before encountering a sensor at the channel's end for consecutive detection, neurotransmitter separation was accomplished by AC field disruption in a microfluidic channel. Seven NTs (5-hydroxytryptamine, dopamine, norepinephrine, epinephrine, 5-hydroxyindoleacetic acid, 5-hydroxytryptophan, and 3, 4-dihydroxy-L-phenylalanine) were detected by the sensor, which utilized certain electron transfer mediators. The sensor probe was made by combining electropolymerization of 2,2':5',5''-terthiophene-3'-p-benzoic acid (TBA) with heteroatom (N and S)-doped porous carbon (HPC) to create a composite layer. This was then applied onto a SPCE, and a redox mediator was covalently immobilized on top. When compared to the other mediators that were evaluated, Evans blue showed the best performance. To maximize the sensing performance, we fine-tuned the AC parameters (frequency, amplitude, etc.), fluid flow rate, temperature, and pH. The detection limits ranged from 0.034 (± 0.005) to 0.044 (± 0.004) nM, and the calibration plots for the seven NT standard samples were determined to be linear within the range of 0.05–130 nM. Lastly, a human plasma sample was used to identify six NTs and two NT derivatives, evaluating the device's dependability [93]. Ahmad et al. studied the preparation and characterization of nitrogen-doped reduced graphene oxide (N-rGO) utilizing several state-of-the-art techniques, including XRD, SEM, EDX, Raman, and XPS. A screen-printed carbon electrode (SPCE) had its active surface altered by drop-casting N-rGO. When it came to detecting hydrogen peroxide (H_2O_2), this modified electrode (N-rGO/SPCE) showed an outstanding limit of detection (LOD) of 0.83 μM and a respectable sensitivity of 4.34 $\mu\text{A } \mu\text{M}^{-1} \text{ cm}^{-2}$. Furthermore, N-rGO/SPCE demonstrated remarkable stability, reproducibility, and selectivity for H_2O_2 sensing. Additionally, tests on actual samples demonstrated respectable field recovery [137].

Pan et al. created an electrochemical sensor based on a graphene oxide-modified screen-printed carbon electrode for detecting ciprofloxacin (CIP) via its complexation with Mn^{2+} . Food safety relies on the constant monitoring of antibiotic residues in foodstuffs using fast detection methods. Due to the presence of CIP, the anodic stripping peak current response of Mn^{2+} was suppressed on the modified electrode, resulting from a peak current response of the complex. Since the complexation peak's peak current response was more sensitive than CIP's direct electrochemical oxidation response, it was used as an indicating signal for CIP determination. The linear correlation value (R^2) was 0.994, and under ideal conditions, there was a linear relationship between the peak current of the complexation peak and the CIP content in a milk sample solution at concentrations ranging from 1.0 to 8.0 μM , and at 0.30 μM , the LOD was reached. With relative standard deviations (RSDs) < 4.6%, CIP recoveries in milk samples varied from 81.0% to 95.4%. This approach demonstrated promising results for CIP residue analysis, including high selectivity, sensitivity, and reproducibility [138].

Carbon Nanotubes

Carbon nanotubes (CNTs) possess a high aspect ratio, enhanced electrical conductivity, notable chemical stability, and exceptional mechanical strength and electrical properties. These unique properties, along with their enhanced electrical properties, such as facilitating electron transport and possessing a large surface area, attract attention for incorporation into composites or modified electrodes for analytical applications. Furthermore, due to the intrinsic plasticity of carbon surfaces, several investigations employing carbon nanotubes to improve biosensor performance have been conducted [86,139,140]. MWCNTs are porous carbon materials characterized by great chemical and mechanical durability, extensive surface area, and distinctive electrical conductivity, and their integration on SPCE enhances the electronic transfer characteristics of the electrodes, yielding high sensitivity, the lowest detection limits, and reduced overpotentials. These features offer an exceptional modification of SPCEs with MWCNTs [140,141].

Couto et al. described the development, characterization, and application of an electrochemical sensor utilizing Nafion/MWCNT-SPCEs for the voltammetric detection of the anti-tuberculosis medication ethambutol (ETB). The results indicated that negatively charged Nafion/MWCNT-SPCEs significantly improved the electrochemical sensitivity and selectivity for ETB when compared to both unmodified and MWCNT-modified SPCEs. This enhancement is attributed to the synergistic effect of the electrostatic interaction between cationic ETB molecules and the negatively charged Nafion polymer, along with the intrinsic electrocatalytic properties of both MWCNTs and Nafion. Nafion/MWCNT-SPCEs exhibited superior biocompatibility, commendable electrical conductivity, minimal electrochemical interferences, and a high signal-to-noise ratio, facilitating exceptional performance in ETB quantification in microvolumes of human urine and blood serum samples. The findings of this research validate that the Nafion/MWCNT-SPCE-based device may serve as a viable option for creating an economical, dependable, and efficient electrochemical portable sensor for the detection of an antimycobacterial medication at low concentrations in biological samples [86].

Hu et al. created an electrochemical sensor that can detect menthone, a biomarker linked to epilepsy seizures. The menthone-based electrochemical sensor is built upon a SPCE that has been modified with a nanomaterial of $\text{Cu}_2\text{O@MWCNTs}$. The electrode has a sensitivity of $88.243 \mu\text{A} \cdot \text{mM}^{-1} \cdot \text{cm}^{-2}$ and a detection limit of 0.3 mM. Furthermore, the SPCE/ $\text{Cu}_2\text{O@MWCNTs}$ electrode showed a strong linear relationship with the concentration of menthone in PBS. The outstanding biocompatibility of the SPCE/ $\text{Cu}_2\text{O@MWCNTs}$ electrode was further confirmed by the cell assay findings, showing its potential for use in real biosamples [142]. Araujo et al. assert that SPCEs may be fabricated using cost-effective materials. The carbon conductive ink they used was composed of graphite powder and transparent nail polish. To fabricate SPCEs, ink was deposited onto flexible, water-resistant polyester overhead projector sheets, and MWCNTs were drop-cast to improve the analytical efficacy and electrochemistry of SPCE. MWCNT/SPCEs were used to quantify caffeic acid (CA) in tea samples, and they exhibited the most extensive linear range for CA, spanning from 2.0 to $50 \mu\text{mol L}^{-1}$. Furthermore, these MWCNTs exhibited low detection and quantification thresholds of 0.20 and $0.66 \mu\text{mol L}^{-1}$, respectively. The electrodes demonstrated recovery rates of 99–109% for tea samples, accompanied by low relative standard deviation values, thus validating the accuracy of the proposed sensor. The novel SPCE enabled voltammetric measurements with just 100 μL of solution, making it both economical and ecologically sustainable [143].

6.2.4. Modification by Polymers

A polymer is a long-chain substance made up of many units that have the same structure and repeat. Some polymers, like proteins, cellulose, and silk, are found in nature. Other polymers, like polystyrene, polyethylene, and nylon, can only be made in a lab. Polymeric materials are used in almost every part of daily life [144]. Among them, conducting polymers (CPs) are organic substances that exhibit not only superior electrical conductivity, but their mechanical characteristics also do not align with those of other commercially available polymers, and they also have a wide range of remarkable features, including magnetic, optical properties, microwave-absorbing properties, and wetting in electrochemical sensors that have garnered significant interest because of their electroactivity. Examples include polypyrrole, polyaniline, polythiophene, and poly-beta cyclodextrin (p-beta-CD), based on the findings of leading researchers, owing to their superior electrochemical characteristics and straightforward production. The electrical characteristics may be optimized by synthetic procedures and sophisticated dispersion techniques. Synthesized nanostructures of conducting polymers are particularly intriguing due to their characteristics, which markedly differ from those of their bulk counterparts, and they are great options for electrode modification. CPs are used in many areas today, such as healthcare and energy storage [89,123,145–147].

Karbelkar et al. used the cyclic voltammetric reduction in aniline on SPCE, and the aniline-modified electrodes with a surface coverage of roughly 2 nmol cm^{-2} were quite stable once altered, and they were simpler to manufacture than SAMs on a gold electrode [24]. Raj et al. developed a sensitive electrochemical approach to detect dopamine (DA) and 5-hydroxytryptamine (5-HT) simultaneously, utilizing graphene (GR) and a poly(4-amino-3-hydroxy-1-naphthalenesulfonic acid)-modified SPCE. Electrochemical measurements were conducted using CV and SWV, while the surface morphology of the modified sensor was documented using EIS and field-emission scanning electron microscopy (FE-SEM). The constructed sensor could analyze DA and 5-HT at 0.05–100 M and 0.05–150 M with detection limits of 2 nM and 3 nM, respectively. The manufactured sensor was tested for detecting 5-HT in plasma samples, demonstrating selectivity by analyzing DA and 5-HT in the presence of common metabolites in biological fluids [148]. Filik et al. proposed the use of magnetic solid phase microextraction coupled with electrochemical detection for the analysis of caffeine in chocolate milk, soft drinks, and energy beverages. SPCE modified with poly(Alizarin Red S) served as an electrochemical sensor. The viability of magnetic solid-phase microextraction for electroanalytical methods such as SWV remains ambiguous. Under optimal conditions, the system response exhibited a direct proportionality to caffeine concentrations between 0.5 and 20 μM , with a correlation coefficient of around 0.9987. The sensor has a detection limit of 0.05 μM [149].

6.2.5. Modification Using Molecularly Imprinted Polymers (MIP)

Synthetic versions of the natural, biological antibody–antigen complexes are called molecularly imprinted polymers, or MIPs. This means that they attach to their template molecule selectively, much like a “lock and key” process, as shown in Figure 7. MIPs have the selectivity and specificity of biological receptors with the obvious benefits of low cost and high endurance in harsh environments [150]. Since electrochemical sensors are highly sensitive, portable, and respond quickly, they have found widespread use in the detection of biological and pharmacological analytes. At present, the MIPs utilized in electrochemical sensors can be synthesized through several methods, including the drop-coating method, which involves applying MIP suspensions onto the surface of electrodes, as well as chemical polymerization and electrochemical polymerization.

To make MIPs, functional monomers containing the target analyte (the template) and a crosslinker are first polymerized. Then, to create binding sites with high fidelity, the template is removed. The resulting polymers are very versatile, inexpensive, reusable, and chemically and physically stable, making them ideal for use in a wide range of sensing applications. Electrochemical polymerization is quickly replacing other methods for creating molecularly imprinted electrochemical sensors because the resulting MIPs have a film thickness that can be controlled and sufficient adhesion strength to the electrode surface. Electropolymerization is the synthesis method of choice for producing electrochemical sensors based on MIPs. It is worth noting that MIP-based sensors have multiple purposes: first, they bind target molecules selectively; second, they translate binding events into quantifiable electrochemical signals; and last, they act as recognition elements. Several areas have shown promising results using these sensors, such as environmental monitoring, bioimaging, therapeutic diagnostics, artificial antibodies, immune-type assays, and food safety. Many different analytes have been detected using MIPs. These include peptides, proteins, and even entire cells, as well as smaller molecules like cortisol, hormones, pesticides, carbohydrates, amino acids, and medications. Compared to many naturally occurring biorecognition elements, MIPs outperform them due to their high selectivity, affinity, and stability across a wide variety of physical and chemical environments. They are highly advantageous as next-generation recognition materials for selective and sensitive electrochemical sensing of both small and large molecules due to their flexibility in complicated media, low cost, and absence of dependence on components generated from animals. This includes biological fluids and environmental samples [3,85,90,151–153].

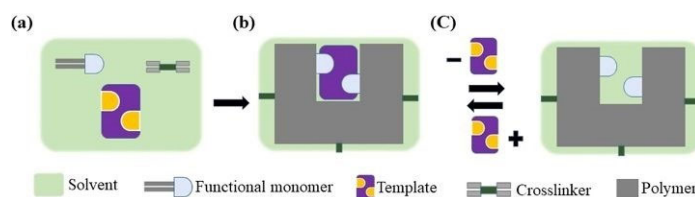


Figure 7. Diagrammatic illustration of the procedures involved in MIP preparation. (a) A pre-polymerization mixture made up of a solvent-dissolved cross-linker, functional monomer, and template. (b) During polymerization, a polymeric network combined with the template molecule is formed. (c) Rebinding the template (analyte) after it has been removed (extracted) to generate and assess cavities. Reproduced from ref. [154], with permission from Wiley Online Library, copyright 2024.

Ting W. et al. developed an interleukin-6 (IL-6) anchoring platform for electrochemical sensing utilizing MIP. O₂ plasma treatment, Au electrodeposition, APTES and GA modifications, and SPCE immobilization of IL-6 were all part of a well-defined procedure. Improving the platform's IL-6 imprinting efficiency by surface functionalization to aid IL-6 embedding, IL-6 removal, and IL-6 rebinding efficiency testing was the primary goal of this work. It is encouraging to note that the as-prepared MIP showed increased surface energy, roughness, and weaker mechanical strength compared to NIP, which indicated the presence of IL-6 within poly(o-phenylenediamine). The MIP sensor's sensitivity and selectivity were thoroughly tested. With a limit of detection (LOD) of 1.74 pg mL⁻¹, the improved MIP sensor showed a strong response to IL-6 concentrations ranging from 2 to 400 pg mL⁻¹. It was highly specific for IL-6 and showed very little cross-reactivity. Due to its improved anchoring and selective detection, the created MIP-based IL-6 sensor shows potential for use in clinical settings. Improved IL-6 diagnostics could influence illness monitoring due to this newly created sensor. The performance of the sensor in real-world clinical practices could be improved with more application research and refinements [94].

Zhou L. et al. developed a wearable amperometric sensor based on MIP/Ag-Au NPs/SPCE for lactate sweat analysis in healthcare and sports. MIPs were formed via electropolymerization on the surface of SPCE after spin-coating the chemically produced Ag and Au NPs. Structural and morphological investigations revealed a uniform distribution of spherical Ag-Au nanoparticles on MIP molecules. Electrochemical studies showed that adding MIP particles to Ag-Au NPs increased surface electroactive sites, improving stability, selectivity, and analytical signal through direct electron transfer between the substrate and electrochemical ions. Lactate sensor's linear range, detection limit, and sensitivity were 1–220 μM , 0.003 μM , and 0.88066 $\mu\text{A } \mu\text{M}^{-1}$, respectively. The suggested flexible sensor showed high endurance and stability under mechanical stresses, including twisting and bending. MIP/Ag-Au NPs/SPCE sensor was mounted to the volunteers' skin to measure lactate levels during cycle activity. The results indicated that this wearable sensor is viable and reliable for continuous lactate monitoring in sweat [100]. Khosrokhavar et al. created a new electrochemical sensor that selectively detects the antidepressant sertraline (STR) using a molecularly imprinted polymer (MIP) through the precipitation polymerization process, with sertraline hydrochloride serving as the template molecule. To create the sensor, screen-printed carbon electrodes (SPCEs) that were handmade were coated with a very thin coating of MIP/graphene suspension, as shown in Figure 8. The sensor was characterized using cyclic voltammetry and differential pulse voltammetry techniques, with the $\text{K}_3[\text{Fe}(\text{CN})_6]/\text{K}_4[\text{Fe}(\text{CN})_6]$ redox pair serving as a probe. Compared to the non-imprinted polymer (NIP)/graphene-modified SPCEs, the MIP/graphene-modified SPCEs demonstrated superior adsorption performance in the sertraline binding assays. We tuned the extraction pH, preconcentration time, sample solution stirring rate, MIP/graphene suspension composition, and other factors that impact the sensor response. In ideal settings, the sensor showed a high level of sensitivity ($177.25 \mu\text{A L } \mu\text{mol}^{-1}$) to sertraline, with a linear range of 5.0×10^{-9} to 7.5×10^{-7} M ($R^2 = 0.9971$) and a detection limit of 1.99×10^{-9} M. Sertraline was accurately measured in both tablet and human serum samples using the sensor, with recovery values ranging from 97.98 to 101.33% [85].

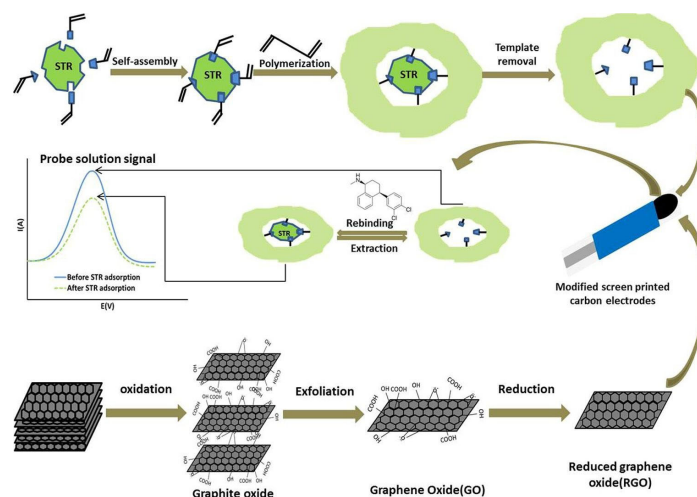


Figure 8. SPCE modified with MIP and graphene for detection of the antidepressant drug sertraline (STR) using DPV. Reproduced from ref. [85], with permission from Elsevier, copyright 2020.

6.2.6. Modification by Composite Nanostructures

Any solid substance that consists of multiphases, with at least one phase having one, two, or three dimensions at the nanoscale, is called a nanocomposite. The aim of achieving synergy between various components is accomplished via the nanoscale phase process. Nanoparticles, nanofibers, and nanoclays are the nanomaterials that make up

almost all nanocomposites. Future materials will likely include nanocomposites [155,156], which provide an alternative to microcomposites and monolithics. The primary benefits of nanocomposites compared to other composite materials are improved mechanical properties, including high ductility without strength loss and scratch resistance; improved optical properties, including light transmission depending on particle size; improved electrical conductivity, and a high surface/volume ratio that permits small filler size and less distance between fillers [156–159].

Saengsookwaowa et al. made a screen-printed carbon electrode (SPCE) with nitrogen-doped graphene (NG)-polyvinylpyrrolidone (PVP)/gold nanoparticles (AuNPs) to measure hydrazine using SWV. To modify the electrode, NG-PVP nanocomposites were electro-sprayed onto the SPCE surface, and then AuNPs were added electrochemically on top of the NG-PVP nanocomposite layer. The electrode composition and SWV settings, which affect how sensitive the sensor is, were improved. CV, SEM, TEM, and EIS were used to study the physical and chemical properties of modified SPCEs. Because NG-PVP and AuNPs work together, the adjusted SPCE had a 10-times higher anodic peak current than an SPCE that was not changed, which shows that the system is very sensitive. Additionally, this system showed excellent electrocatalytic activity for oxidizing hydrazine. For hydrazine, the best conditions led to a wide linear range of 2–300 M, a low detection limit of 0.07 M, and a high sensitivity of $1.370 \text{ A M}^{-1} \text{ cm}^{-2}$. It is interesting that this method worked very well against a range of sugars, like glucose, sucrose, and lactose. It seems that this is the first report on how NG-PVP/AuNPs-tweaked SPCE was successfully created and used to detect hydrazine in samples of high-sugar fruits and vegetables [97].

Haddaoui et al. developed zinc oxide nanoparticles electrochemically and nanostructured tyrosinase-modified SPCEs, which constituted the sensing platform. Scanning electron microscopy, electrochemical impedance spectroscopy, and cyclic voltammetry were used to evaluate the progressive surface alteration. With a sensitivity of 18.71 nA M^{-1} and a limit of detection of 0.02 M, the modified electrode can selectively detect phenol ranging from 0.1 to 14 M. The presence of chlortoluron inhibits enzyme activity in a concentration-dependent manner. With an inhibitory level range of 1 to 100 nM and a limit of detection of 0.47 nM ($\sim 0.1 \text{ ppb}$), the biosensor demonstrates a linear relationship ($r > 0.998$) [96]. Ibanez-Reddin et al. formulated a sustainable method for synthesizing carbon black (CB) and electrochemically reduced graphene oxide composite (ERGO) using SPCEs constructed on poly (ethylene terephthalate) (PET) as electrochemical sensors. This method resulted in a heterogeneous hydrophilic surface. The SPCE/CB-ERGO sensor was evaluated with dopamine (DA), epinephrine (EP), and paracetamol (PCM), demonstrating superior electrocatalytic performance relative to the unmodified SPCE. It exhibited an expanded linear range, reduced limit of detection, and significantly enhanced analytical sensitivity, which are 1.5, 0.13, and $0.028 \text{ A L mol}^{-1}$ for DA, EP, and PCM, respectively, while also facilitating the simultaneous quantification of the three analytes [160].

Wu et al. created an easy-to-carry and lightweight electrochemical sensor for finding As (III) using a modified SPCE made by stepwise electrodeposition of reduced graphene oxide, gold nanoparticles, and manganese dioxide (rGO/AuNP/MnO₂). The electrode's shape, structure, and electrical features were measured using SEM, XPS, EDX, CV, and EIS. The shape of the material shows that AuNPs and MnO₂ were deposited thickly or trapped in thin rGO sheets on the porous carbon surface. The nanohybrid lowers the resistance to charge transfer and raises the electroactive specific surface area, which makes the As (III) electro-oxidation current much stronger. When As (III) is reduced electrochemically, gold nanoparticles with great electrocatalytic properties and rGO with good electrical conductivity work together to make detection better. Manganese dioxide, which has a strong ability to absorb things, also played a part. As (III) can be found using square wave

anodic stripping voltammetry (SWASV), and the sensor has a linear range of 25–200 $\mu\text{g L}^{-1}$ and a low limit of detection of 2.4 $\mu\text{g L}^{-1}$. The suggested portable sensor is easy to set up, cheap, repeatable, and stable over time [161].

7. Comparative Analysis of Using Unmodified SPCE vs. Modified SPCE

A comparative analysis of many screen-printed electrodes modified with electrochemically reduced graphene oxides or partially reduced graphene oxides exhibiting various morphologies through galvanostatic reduction was conducted. The analysis indicated that galvanostatic reduction, which involves the application of current for a specified duration, is an effective electrochemical method for reducing graphene oxide, particularly when utilizing screen-printed electrodes with a pseudo-reference electrode. It was shown that electrodes treated with graphene oxides containing increased acid groups had a greater electroactive area, enhanced reversibility, accelerated kinetics, and elevated double-layer capacitance. While these parameters can significantly affect the analytical determination of various species, the optimal analytical characteristics (maximum sensitivity) for dopamine were achieved using graphene oxide that had been treated with hydrazine. This observation suggests that the interaction between the analyte and graphene may be more critical for the analytical determination than the enhancement of electrochemical properties (such as electroactive area and accelerated kinetics), which shows that varying graphene materials and reduction conditions can serve as a mechanism for modulating their electrochemical characteristics [162].

8. Use of Modified Screen-Printed Electrodes for Multi-Analyte Detection

SPCEs may be used to detect multiple analytes simultaneously. In some cases, this is possible because the analytes have sufficiently separated oxidation potentials. In other cases, SPCEs with more than one working electrode printed onto the substrate are used. SPCEs with more than one working electrode are needed if there are specific recognition molecules, such as monoclonal antibodies, to be immobilized on the working electrodes, which are unique to each analyte. SPCEs were modified with a calixarene to improve the sensitivity for binding and simultaneous detection of Pb(II), Cu(II), and Hg(II) ions through coordination to hydroxyls around the upper rim of the molecule [163]. The calixarene was incorporated into the ink used to print the working electrode. The bound metal ions were reduced to -1.1 V (vs. Ag/AgCl) and then detected by differential pulse anodic stripping voltammetry (DPASV). The oxidation potentials of the metals were clearly separated so that detection could take place simultaneously. A wide linear range of up to 2400 mg L^{-1} was observed with detection limits of 38, 40, and 49 mg L^{-1} for Pb(II), Cu(II), and Hg(II), respectively. Modification of SPCEs with an electrodeposited layer of Bi/Hg aimed at increasing the sensitivity was used for simultaneous detection of Zn(II), Cd(II), Pb(II), and Cu(II) [164]. The modification reduced R_{ct} from 661 $\text{k}\Omega$ to 6 $\text{k}\Omega$, as determined using EIS. The metal ions were then reduced and detected using square wave anodic stripping voltammetry (SWASV) over the range -1.3 to 0.5 V . Low detection limits of 0.97, 0.16, 0.27, and 2.14 ppb were found for Zn(II), Cd(II), Pb(II), and Cu(II), respectively. The simultaneous detection of the pesticides carbaryl (CBR), fenobucarb (FNB), and carbosulfan (CBS) was achieved using SPCEs modified with a MnO_2 nanoparticles/graphene nanoplatelets composite via drop-casting [165]. MnO_2 nanoparticles were used as they are good for detecting phenolic compounds, with high electrocatalytic activity and reduced overpotential for oxidation of these compounds. DPV was used, and the oxidation potentials of 0.17 V, 0.40 V, and 0.90 V (vs. C reference) were well separated. Detection limits of 0.3, 1.40, and 15.15 mM were found for CBR, FNB, and CBS, respectively. Agreement with HPLC determinations was excellent for spiked samples. Simultaneous detection of the antibiotics sulfamethoxazole

(SMX) and trimethoprim (TMP), used together to treat infections, was reported using SPCEs modified by MWCNT decorated along their edges with 50 nm Prussian blue (PB) nanocubes [166]. PB nanocubes serve as mediators and electrocatalysts. On the modified SPCE, the oxidation peak potential was at 0.575 V for SMX and 0.740 V for TMP (vs. Ag/AgCl), and both could be detected together with detection limits of 38 nM and 50 nM, respectively. Recovery of each sample spiked in artificial urine was excellent. In the simultaneous detection of antibiotics linomycin and neomycin on SPCEs, a dual SPCE was used since aptamers binding to these two antibiotics were separately immobilized together in a Au nanoparticle/carbon nanofiber composite [167]. SWV was used to follow the decrease in the peak current associated with $\text{Fe}(\text{CN})_6^{3-/4-}$ oxidation upon analyte binding. For linomycin, the linear range was 0.005–406.5 pg mL^{-1} with a detection limit of 0.065 pg mL^{-1} . For neomycin, the linear range was 0.01–1000 pg mL^{-1} with a detection limit of 0.02 pg mL^{-1} .

For many diseases, there are multiple complementary biomarkers, and hence, simultaneous detection of more than one can be useful, and SPCEs with multiple specifically modified working electrodes make this possible. In one of the earlier such studies, biomarkers carcinoembryonic antigen (CEA), alpha-fetoprotein (AFP), beta human chorionic gonadotropin (b-hCG), and cancer antigen—125 (CA-125) were detected simultaneously using SPCEs in a flow-injection apparatus [168]. The working electrodes were modified by chitosan, to which the redox mediator toluidine blue O was covalently attached. Each working electrode was modified by one of the biomarkers by drop-casting. Using horseradish peroxidase-labeled antibodies on each biomarker, competitive immunoassays were established. Amperometry was used to monitor the H_2O_2 produced, and the current decreased proportionately to biomarker concentration. Linear ranges of up to 188 kIU L^{-1} , 250 kIU L^{-1} , 266 kIU L^{-1} , and 334 kIU L^{-1} were found for CEA, AFP, b-hCG, and CA-125, respectively. Detection limits of 1.1 kIU L^{-1} , 1.7 kIU L^{-1} , 1.2 kIU L^{-1} , and 1.7 kIU L^{-1} were found, respectively. The sensor was found stable for 28 days. The tumor biomarkers carcinoembryonic antigen (CEA) and alpha-fetoprotein (AFP) were detected together using SPCEs and a nanoparticle-based strategy [169]. Gold nanoparticles were labeled with monoclonal antibodies (MAb) against these two proteins, one for binding CEA and another for binding AFP. The Mabs were also immobilized onto the SPCE working electrodes in a chitosan matrix to which they were cross-linked using glutaraldehyde. After incubation with the biomarker in a 15 mL drop, Au nanoparticles bearing Mab were allowed to bind. Finally, the bound Au nanoparticles were used as nucleation sites for the electrodeposition of Ag. LSV was applied to oxidatively strip off the Ag, and the peak current was proportional to the log10 of the biomarker concentration over the range 5 pg mL^{-1} to 5 ng mL^{-1} with detection limits of 3.5 pg mL^{-1} and 3.9 pg mL^{-1} for CEA and AFP, respectively. In a later study, the tumor markers cytochrome c (CYC) and vascular endothelial growth factor 165 (VEGF-165) were detected together using SPCE with two working electrodes, each modified by a different aptamer [170]. Reduced graphene oxide and Au nanoparticles were dropcast onto the working electrodes in a dendrimer matrix. Glutaraldehyde was used to link flavin adenine dinucleotide as a redox marker to one working electrode and thionine as a redox marker to the other working electrode. The aptamers for CYC and VEGF-165 were then applied to different working electrodes. Upon binding of the biomarker protein(s), the peak current from the redox probes in a DPV scan decreased with DI proportional to the biomarker concentration. The standard potential for the two redox probes versus the Ag reference was well separated, with -0.589 mV for FAD and -217 mV for thionine. Detection limits of 1.0 pM for CYC and 0.7 pM for VEGF-165 were obtained. After 14 days of storage in PBS, the sensor peak current diminished by 4.5%. Electrochemical multi-analyte detection in the broader sense has been reviewed [171]. SPCE with two working electrodes

was used to simultaneously detect cancer antigen 15-3 (CA 15-3) and human epidermal growth factor receptor 2 (HER2-CD), both of which are biomarkers for breast cancer [172]. The SPCE working electrodes were modified by electrodeposition of Au nanoparticles, and then MABs for the biomarkers were applied separately to each working electrode. After capturing the biomarker, alkaline phosphatase (ALP)-labeled versions of each MAB were applied. ALP acting on 3-indoxylphosphate and dissolved silver nitrate produced metallic silver that was detected using LSV. For CA 15-3, a linear range of 0–70 U mL⁻¹ was achieved with a detection limit of 5.0 U mL⁻¹, and for HER-ECD, a linear range of 0–50 ng mL⁻¹ was achieved with a detection limit of 2.9 ng mL⁻¹. A dual SPCE approach was also reported for the detection of receptor activator of nuclear factor- κ B ligand (RANKL) and tumor necrosis factor alpha (TNF), which are two newer biomarkers for breast cancer [173]. Magnetic beads were functionalized with biotinylated capture MABs and applied to each working electrode. After biomarker binding, detector MABs were allowed to bind, followed by the binding of anti-mouse IgG labeled with HRP. The current from the oxidation of H₂O₂ in the presence of benzoquinone mediator was measured. Detection limits of 2.6 and 3.0 pg mL⁻¹ were found for RANKL and TNF, respectively. Samples from both healthy patients and those with breast cancer showed good agreement with ELISA measurements of biomarker concentrations. Dual SPCEs and magnetic beads were also used to simultaneously detect protein IL-8 and its messenger RNA, which are biomarkers for oral cancer [174]. The beads were modified with MAB for binding IL-8, and another group of beads was modified by a specific hairpin DNA sequence to capture IL-8 mRNA. Detection was also based on oxidation of H₂O₂ by HRP-labeled detection MAB or by an HRP-streptavidin bound to a biotinylated strand. Detection limits of 0.21 nM and of 72.4 pg mL⁻¹ were found for IL-8 mRNA and IL-8, respectively. Good agreement was found for determinations in saliva from healthy volunteers with that found using ELISA kits. A later study using magnetic beads in immunocomplexes developed SPCE to simultaneously detect three biomarkers associated with ovarian cancer [175]. Mesoporous silica nanoparticles were combined with either Au nanoparticles, PbS quantum dots, or CdTe quantum dots conjugated with secondary antibodies and were used for detection by applying square wave anodic stripping voltammetry to detect the three metals at unique potentials. The SPCE used was modified by a bismuth film to increase the sensitivity. The biomarkers for esophageal cancer tumor protein 53 (TP53) and cytokeratin fragment 21-1 (CYFRA21-1) were detected simultaneously using SPCE printed on paper [176]. The antibodies against these biomarkers were immobilized by drop-casting. Detection was achieved using CV and the reduction in peak current for Fe(CN)₆^{3-/4-} upon biomarker binding, achieving limits of detection of 0.012 ng mL⁻¹ and 0.005 ng mL⁻¹ for TP53 and CYFRA21-1, respectively.

A newer development in multi-analyte detection on SPCE has been the introduction of machine learning strategies. A good example is the application of machine learning to an aptasensor developed for simultaneous detection of di(2-ethylhexyl) phthalate (DEHP) and bisphenol A (BPA) [177]. The SPCE was modified by gold nanoflowers and achieved detection limits using DPV for DEHP and BPA of 0.58 and 0.59 pg mL⁻¹, respectively. The DPV response varies with pH, and thus testing at rivers of different pH was a challenge overcome by the introduction of machine learning by the least-squares boosting algorithm. Calibration plots at pH values from 4.5 to 10.5 were used. Detection in water samples from 12 locations around South Korea provided results within 6% or better agreement, with the analysis performed using liquid–liquid extraction/gas chromatography/mass spectrometry (LLE-GC-MS).

9. Greener and More Sustainable Methods for Producing SPCEs

Attention has grown in recent years to the goal of producing greener and biodegradable SPCEs so that they will pose less of an environmental burden when disposed of. Polyethylene terephthalate (PET), reused from plastic bottles, was used as the substrate for SPCEs made using a low-cost ink made by combining nail polish and graphite powder. The sensor was used for the detection of hydroquinone (HQ), an environmental pollutant, and neurotransmitters epinephrine (EP) and serotonin (5-HT) using SWV for EP detection and DPV for the detection of EP and 5-HT, with sub-micromolar detection limits achieved [178]. The same ink was later used on a polyvinyl chloride (PVC) support to make an SPCE for the detection of levofloxacin [179]. In another example, flexible fiber mats of polylactic acid (PLA) and polyethylene glycol (PEG) were spun and used as the substrate for an SPCE onto which glucose oxidase was covalently attached along with Prussian blue nanoparticles. The biosensor detected hydrogen peroxide produced by the oxidation of glucose and was tested in synthetic and human urine, providing a detection limit of 0.197 mM and a range of 1.0–6.0 mM. The cost of the biosensor was less than USD 0.25 [180]. SPCEs using the biodegradable polymer, polylactic acid, as the support have been reported and used to develop a sensor for simultaneous detection of dopamine and uric acid using DPV. The Sensit handheld, wireless potentiostat from Palmsens was used. Detection was studied in both artificial urine and human urine samples from healthy volunteers. Good selectivity and recovery were achieved with detection limits of 0.138 mM for dopamine and 0.595 mM for uric acid [181]. Recently, silk fibroin was introduced as a bioabsorbable substrate so that an SPCE sensor could be made implantable for use as a glucose sensor that would ultimately be absorbed by the body through digestion by enzymes [182]. The application and curing of carbon paste created the carbon working electrode. A number of modifications were explored, including O₂ plasma treatment with MWCNT. The modification with MWCNT and glucose oxidase with BSA and cross-linker glutaraldehyde in glycerol produced a sensor that responded to glucose concentration. A Palmsens3 potentiostat was used for the sensor evaluation, and a linear range of up to 4 mM was found, with the best limit of detection of 0.4 mM at 1.0 V (vs. Ag/AgCl). In the presence of a protease, the sensor was fully degraded within 63 days. Screen-printing of carbon composites on ethyl cellulose paper was investigated, and the best result, in terms of adhesion, durability under bending, and surface resistance (below 1 kW/square), was found for an 8 wt% ethyl cellulose solution with 8 wt% graphene, cured on paper at 120 °C [183]. The field of paper-based sustainable biosensors has recently been reviewed [184], and reference is made to a SPCE modified with a cellulosic paper disk modified with glucose oxidase for sensing glucose concentration in beverages [185]. An ink used to make a carbon paste electrode was made using recycled acrylonitrile butadiene styrene (ABS) pieces leftover from the use of the 3D-printing material for substrates. The ink was made by dissolving ABS fragments in acetone/chloroform and adding graphite. The result was applied as a sensor for the drug acebutolol [186]. The ecologically friendly and biodegradable substrates of paper, silk fibroin, and polylactic acid hold significant promise for developing disposable SPCEs with low environmental impact. The field of ecologically friendly screen-printed electrodes has been reviewed in a recent book chapter [187].

10. Advances in Integrating Modified SPCEs for Wearable Sensors

Modification of SPCEs is crucial for their successful use in wearable sensors. These wearable sensors are in various stages of intense commercial development. Monitoring of sweat for concentrations of electrolytes (Na⁺, K⁺, Cl[−]), metabolites (glucose, lactate, uric acid), and hormones (cortisol) is a prominent goal. Application to other biomarkers is also an area of intense interest. The successful application of SPCE in wearable sensors also

requires their surface to be modified to improve sensitivity, selectivity, and stability. A significant amount of development has focused on wearable lactate sensors. Lactate oxidase (LOx) was drop-cast onto a working electrode made by printing a carbon black/Prussian blue suspension onto flexible polyester film [25]. Lactate oxidase converted lactate into pyruvate and generated H_2O_2 that could be detected amperometrically. The Sensit Smart portable potentiostat was used for measurements. A linear range from 0.1 to 20 mM and a detection limit of 60 nM was found, with little interference from uric acid, dopamine, or glucose. Validation using real sweat samples was successful, and then the biosensor was incorporated into a wearable armband, and the lactate measurements agreed well with those found by LC-MS/MS. MXene nanostructures are promising for surface modification of SPCE due to their high conductivity and high surface area, and variable chemistry. SPCE was modified by MXene $\text{Ti}_3\text{C}_2\text{T}_x$ (T_x are functional groups -OH, -F, O, and -Cl on the surface of the Ti, [188]) and polydopamine and Ag nanoparticles that served to prevent restacking of MXene layers. Finally, LOx was dropcast together with chitosan as an anti-interference layer. The sensor was on a printed circuit board to be worn on the arm, and an Android app was used to measure the current response due to lactate from human sweat during exercise [189]. Over 30 days, the current response was seen to decline by about 16%. A linear range of 5–15 mM was reported with a detection limit of 0.181 mM. Glucose is another analyte of high interest for wearable sensors based on SPCEs. For wearable sensors, glucose can be detected in interstitial fluid. SPCE modified with Prussian blue, with an added layer of nickel hexacyanoferrate, followed by glucose oxidase (GOx)/BSA covered in Nafion, was integrated with a hollow microneedle array and a microfluidic tube for glucose measurements on skin [190]. The Nafion was needed to reduce diffusion and increase the high end of the linear range to levels that need to be followed for diabetic patients. It was noted that the BSA stabilized the GOx, nickel hexacyanoferrate stabilized the Prussian blue redox mediator layer, and Nafion helped limit biofouling. The sensor was demonstrated to work on porcine skin and covered the physiological range of glucose from 2.5 to 22.5 mM. Glucose detection in sweat has also been pursued using SPCE modified by GOx/BSA in chitosan and covered by Nafion [191]. The working electrode was printed from a Prussian blue/carbon paste onto a textile substrate. The range of glucose in sweat is noted as 0–1 mM, which is less than that in interstitial fluid. The sensor produced a linear current response from 20 to 1000 nA. Worn on a person, it observed an increase in glucose in sweat after a meal and exercise. The sensor was subjected to 400 bending cycles, and the current changed by less than 15%; the sensor was stable for 30 days of storage at 4 °C.

11. Conclusions and Future Outlook

SPCEs are a big step forward in electrochemical sensing since they are inexpensive, easy to use, and can be used in many ways. Their incorporation into disposable, portable systems enables applications in point-of-care diagnostics, environmental monitoring, and industrial oversight. Surface modifications, including plasma functionalization, nanomaterials (e.g., AuNPs, graphene oxide, CNTs), polymer composites, and MIPs, substantially boost SPCE performance by augmenting electrocatalytic activity, selectivity, and signal-to-noise ratios. MXenes are becoming more widely used, given their high conductivity and variable surface chemistry. These changes fix some of the problems that unmodified SPCEs have, like lower sensitivity and more susceptibility to interference. This makes it possible to detect analytes at levels as low as nM (for example, heavy metals, neurotransmitters, and viruses). Electrochemical methods like SWV, DPV, and EIS make detection even better by enabling quick, sensitive measurements, even in complex mixtures like biological fluids. SPCEs show great repeatability and flexibility, although there are some problems with reference electrode stability and cross-reactivity.

In terms of scientific and engineering perspectives, the modification of SPCEs faces several key challenges irrespective of their advantages. The main issue is reproducibility and stability originating from non-conductive polymer binders creating heterogeneous surfaces, inconsistent electroactive site density, and variable electron transfer resistance between batches. It is difficult to scale and uniformly deposit nanomaterials via drop-casting, often resulting in non-homogeneous films. Surface fouling, modifier leaching, and shortened shelf life of the modified SPCE make it extremely difficult to achieve durability. Analytes that themselves undergo electropolymerization or strong adsorption pose challenges to overcome, perhaps by developing methods to stabilize them in solution as monomers. High selectivity and managing interference in complex samples, such as blood or saliva, are difficult to achieve due to the presence of nonspecific binding and interferents that readily adsorb onto the surface. It will be important to develop anti-fouling coatings based on polymers that also do not cause reduced signals. Finally, the high-performance modifications usually depend on costly noble metals and complex processes, which conflict with the disposable and low-cost nature of SPCEs.

To overcome these restrictions, future research must focus on proactively addressing critical gaps. A primary focus is the seamless integration with wearable and flexible electronics, necessitating the creation of durable, stretchable conductive inks and a comprehensive understanding of how mechanical stress influences the electrochemical performance and adhesion of modified layers under real-world conditions. These efforts are important for expanding the use of SPCE in wearable devices that can operate in variable environments and remain chemically and mechanically stable. The practical and attractive devices will also need to have an adequate shelf life. Moreover, achieving multi-analyte detection on a singular miniaturized platform requires the investigation of hybrid alterations alongside sophisticated machine learning techniques to decipher intricate electrochemical signals.

Future work on the modification of SPCE should focus on optimizing nanocomposite designs, enhancing reproducibility, and creating wearable/portable sensors for point-of-care applications through the integration of eco-friendly materials, artificial intelligence, and multiplexed systems. The surface modification of SPCEs remains an active area of research to develop high-performance, low-cost electrochemical sensors for various analytical applications, which can be resolved by people from engineering production, electrochemistry, and material science. Future work should concentrate on improving the designs of nanocomposites, enhancing wearable integration, and simplifying the process of manufacturing them so that they can be sold to more people. SPCE-based sensors will continue to be essential for sustainable, real-time analytical solutions in global health and environmental sectors as research continues to improve modification methods and multi-analyte detection.

Author Contributions: Conceptualization: N.H. and K.J.S.; writing—original draft preparation: N.H.; writing—review and editing: N.H. and K.J.S. All authors have read and agreed to the published version of the manuscript.

Funding: This research received no external funding.

Institutional Review Board Statement: Not applicable.

Informed Consent Statement: Not applicable.

Data Availability Statement: No new data were created in the preparation of this review article.

Conflicts of Interest: The authors declare no conflicts of interest.

References

- Baranwal, J.; Barse, B.; Gatto, G.; Broncova, G.; Kumar, A. Electrochemical sensors and their applications: A review. *Chemosensors* **2022**, *10*, 363. [\[CrossRef\]](#)
- Power, A.C.; Gorey, B.; Chandra, S.; Chapman, J. Carbon nanomaterials and their application to electrochemical sensors: A review. *Nanotechnol. Rev.* **2018**, *7*, 19–41. [\[CrossRef\]](#)
- Ibrahim, F.; Sala, A.; Fahs, A.; Morrin, A.; Nanteuil, C.; Laffite, G.; Nicholls, I.A.; Regan, F.; Brisset, H.; Branger, C. Investigation of the modification of gold electrodes by electrochemical molecularly imprinted polymers as a selective layer for the trace level electroanalysis of PAH. *Electrochem. Commun.* **2024**, *169*, 107837. [\[CrossRef\]](#)
- Tiwari, M.S.; Kadu, A.K. Thiol-based chemically modified carbon screen-printed electrode for simultaneous quantification of trace level Pb (II) and Cd (II). *Anal. Sci.* **2024**, *40*, 1449–1457. [\[CrossRef\]](#) [\[PubMed\]](#)
- Reanpang, P.; Themsirimongkon, S.; Saipanya, S.; Chailapakul, O.; Jakmunee, J. Cost-effective flow injection amperometric system with metal nanoparticle loaded carbon nanotube modified screen printed carbon electrode for sensitive determination of hydrogen peroxide. *Talanta* **2015**, *144*, 868–874. [\[CrossRef\]](#)
- Shaikh, M.O.; Srikanth, B.; Zhu, P.-Y.; Chuang, C.-H. Impedimetric immunosensor utilizing polyaniline/gold nanocomposite-modified screen-printed electrodes for early detection of chronic kidney disease. *Sensors* **2019**, *19*, 3990. [\[CrossRef\]](#)
- Kimmel, D.W.; LeBlanc, G.; Meschievitz, M.E.; Cliffler, D.E. Electrochemical sensors and biosensors. *Anal. Chem.* **2012**, *84*, 685–707. [\[CrossRef\]](#)
- Rahmati, Z.; Roushani, M.; Hosseini, H.; Choobin, H. An electrochemical immunosensor using SARS-CoV-2 spike protein-nickel hydroxide nanoparticles bio-conjugate modified SPCE for ultrasensitive detection of SARS-CoV-2 antibodies. *Microchem. J.* **2021**, *170*, 106718. [\[CrossRef\]](#)
- Argoubi, W.; Saadaoui, M.; Aoun, S.B.; Raouafi, N. Optimized design of a nanostructured SPCE-based multipurpose biosensing platform formed by ferrocene-tethered electrochemically-deposited cauliflower-shaped gold nanoparticles. *Beilstein J. Nanotechnol.* **2015**, *6*, 1840–1852. [\[CrossRef\]](#)
- Sedaghat, S.; Kasi, V.; Nejati, S.; Krishnakumar, A.; Rahimi, R. Improved performance of printed electrochemical sensors via cold atmospheric plasma surface modification. *J. Mater. Chem. C* **2022**, *10*, 10562–10573. [\[CrossRef\]](#)
- Crapnell, R.D.; Ferrari, A.G.-M.; Dempsey, N.C.; Banks, C.E. Electroanalytical overview: Screen-printed electrochemical sensing platforms for the detection of vital cardiac, cancer and inflammatory biomarkers. *Sens. Diagn.* **2022**, *1*, 405–428. [\[CrossRef\]](#)
- Suresh, R.R.; Lakshmanakumar, M.; Arockia Jayalatha, J.; Rajan, K.; Sethuraman, S.; Krishnan, U.M.; Rayappan, J.B.B. Fabrication of screen-printed electrodes: Opportunities and challenges. *J. Mater. Sci.* **2021**, *56*, 8951–9006. [\[CrossRef\]](#)
- Shahdost-Fard, F.; Roushani, M. Designing of an ultrasensitive BCM-7 aptasensor based on an SPCE modified with AuNR for promising distinguishing of autism disorder. *Talanta* **2020**, *209*, 120506. [\[CrossRef\]](#)
- Wahyuni, W.T.; Putra, B.R.; Fauzi, A.; Ramadhanti, D.; Rohaeti, E.; Heryanto, R. A brief review on fabrication of screen-printed carbon electrode: Materials and techniques. *Indones. J. Chem. Res.* **2021**, *8*, 210–218. [\[CrossRef\]](#)
- Fletcher, S. Screen-printed carbon electrodes. In *Electrochemistry of Carbon Electrodes*; Alkire, R.C., Bartlett, P.N., Lipkowsky, J., Eds.; Wiley-VCH: Weinheim, Germany, 2015; pp. 425–444.
- Reanpang, P.; Chailapakul, O.; Jakmunee, J. Fabrication of a home-made SPCE modified with thionine for determination of hydrogen peroxide. *Chiang Mai J. Sci* **2018**, *45*, 1449–1459.
- Zhao, X.; Zuo, J.; Qiu, S.; Hu, W.; Wang, Y.; Zhang, J. Reduced graphene oxide-modified screen-printed carbon (rGO-SPCE)-based disposable electrochemical sensor for sensitive and selective determination of ethyl carbamate. *Food Anal. Methods* **2017**, *10*, 3329–3337. [\[CrossRef\]](#)
- Haroon, N.; Stine, K.J. Electrochemical detection of hormones using nanostructured electrodes. *Coatings* **2023**, *13*, 2040. [\[CrossRef\]](#)
- Wahyuni, W.T.; Putra, B.R.; Heryanto, R.; Rohaeti, E.; Yanto, D.H.Y.; Fauzi, A. A simple approach to fabricate a screen-printed electrode and its application for uric acid detection. *Int. J. Electrochem. Sci.* **2021**, *16*, 210221. [\[CrossRef\]](#)
- González-Sánchez, M.I.; Gómez-Monedero, B.; Agrisuelas, J.; Iniesta, J.; Valero, E. Highly activated screen-printed carbon electrodes by electrochemical treatment with hydrogen peroxide. *Electrochem. Commun.* **2018**, *91*, 36–40. [\[CrossRef\]](#)
- Jadav, J.K.; Umrana, V.V.; Rathod, K.J.; Golakiya, B.A. Development of silver/carbon screen-printed electrode for rapid determination of vitamin C from fruit juices. *LWT* **2018**, *88*, 152–158. [\[CrossRef\]](#)
- Paimard, G.; Ghasali, E.; Baeza, M. Screen-printed electrodes: Fabrication, modification, and biosensing applications. *Chemosensors* **2023**, *11*, 113. [\[CrossRef\]](#)
- Nesakumar, N.; Berchmans, S.; Alwarappan, S. Chemically modified carbon based electrodes for the detection of reduced glutathione. *Sens. Actuators B Chem.* **2018**, *264*, 448–466. [\[CrossRef\]](#)
- Karbelkar, A.; Ahlmark, R.; Zhou, X.; Austin, K.; Fan, G.; Yang, V.Y.; Furst, A. Carbon electrode-based biosensing enabled by biocompatible surface modification with DNA and proteins. *Bioconjugate Chem.* **2023**, *34*, 358–365. [\[CrossRef\]](#) [\[PubMed\]](#)

25. Iula, G.; Miglione, A.; Kalligosfyri, P.M.; Spinelli, M.; Amoresano, A.; Di Natale, C.; Darwish, I.A.; Cinti, S. On-body electrochemical measurement of sweat lactate with the use of paper-based fluidics and 3D-printed flexible wearable biosensor. *Anal. Bioanal. Chem.* **2025**, *417*, 3825–3834. [[CrossRef](#)] [[PubMed](#)]
26. Okpara, E.C.; Fayemi, O.E.; Sherif, E.-S.M.; Ganesh, P.S.; Swamy, B.K.; Ebenso, E.E. Electrochemical evaluation of Cd²⁺ and Hg²⁺ ions in water using ZnO/Cu₂ONPs/PANI modified SPCE electrode. *Sens. Bio-Sens. Res.* **2022**, *35*, 100476. [[CrossRef](#)]
27. Yamada, H.; Yoshii, K.; Asahi, M.; Chiku, M.; Kitazumi, Y. Cyclic voltammetry part 1: Fundamentals. *Electrochemistry* **2022**, *90*, 102005. [[CrossRef](#)]
28. Roberts, J.G.; Sombers, L.A. Fast scan cyclic voltammetry: Chemical sensing in the brain and beyond. *Anal. Chem.* **2017**, *90*, 490. [[CrossRef](#)]
29. Rafiee, M.; Abrams, D.J.; Cardinale, L.; Goss, Z.; Romero-Arenas, A.; Stahl, S.S. Cyclic voltammetry and chronoamperometry: Mechanistic tools for organic electrosynthesis. *Chem. Soc. Rev.* **2024**, *53*, 566–585. [[CrossRef](#)]
30. Yamada, H.; Yoshii, K.; Asahi, M.; Chiku, M.; Kitazumi, Y. Cyclic voltammetry part 2: Surface adsorption, electric double layer, and diffusion layer. *Electrochemistry* **2022**, *90*, 102006. [[CrossRef](#)]
31. Ji, D.; Liu, L.; Li, S.; Chen, C.; Lu, Y.; Wu, J.; Liu, Q. Smartphone-based cyclic voltammetry system with graphene modified screen printed electrodes for glucose detection. *Biosens. Bioelectron.* **2017**, *98*, 449–456. [[CrossRef](#)]
32. Koç, Y.; Morali, U.; Erol, S.; Avci, H. Investigation of electrochemical behavior of potassium ferricyanide/ferrocyanide redox probes on screen printed carbon electrode through cyclic voltammetry and electrochemical impedance spectroscopy. *Turk. J. Chem.* **2021**, *45*, 1895–1915. [[CrossRef](#)]
33. Roselló, A.; Serrano, N.; Díaz-Cruz, J.M.; Ariño, C. Discrimination of beers by cyclic voltammetry using a single carbon screen-printed electrode. *Electroanalysis* **2021**, *33*, 864–872. [[CrossRef](#)]
34. Herbei, E.E.; Alexandru, P.; Busila, M. Cyclic voltammetry of screen-printed carbon electrode coated with Ag-ZnO nanoparticles in chitosan matrix. *Materials* **2023**, *16*, 3266. [[CrossRef](#)]
35. Mashat, Z.B.A.; Abdullah, F.; Wahab, A.A.; Shakhhih, M.F.M.; Roslan, A.S. Development of non-enzymatic screen-printed carbon electrode sensor for glucose using cyclic voltammetry. *Environ. Toxicol. Manag.* **2022**, *2*, 14–20. [[CrossRef](#)]
36. Venton, J.; DiScenza, D.J. *Voltammetry in Electrochemistry for Bioanalysis*; Patel, B., Ed.; Elsevier: Amsterdam, The Netherlands, 2020; pp. 27–50.
37. Jazi, H.K.; Sarafbidabad, M.; Henda, M.B.; Ahmadipour, M. The effect of laser surface texturing on ZnO/MWCNT nanocomposite modified screen-printed carbon electrode for non-enzymatic glucose biosensor. *Diam. Relat. Mater.* **2025**, *151*, 111845.
38. Crespi, F. Differential pulse voltammetry: Evolution of an in vivo methodology and new chemical entries, a short review. *J. New Dev. Chem.* **2020**, *2*, 20–28. [[CrossRef](#)]
39. Tyszczyk-Rotko, K.; Kozak, J.; Węzińska, A. Electrochemically activated screen-printed carbon electrode for determination of ibuprofen. *Appl. Sci.* **2021**, *11*, 9908. [[CrossRef](#)]
40. Alberto, E.; Bastos-Arrieta, J.; Pérez-Ràfols, C.; Serrano, N.; Díaz-Cruz, M.S.; Díaz-Cruz, J.M. Voltammetric determination of sulfamethoxazole using commercial screen-printed carbon electrodes. *Microchem. J.* **2023**, *193*, 109125. [[CrossRef](#)]
41. Jirasirichote, A.; Punrat, E.; Suea-Ngam, A.; Chailapakul, O.; Chuanuwatanakul, S. Voltammetric detection of carbofuran determination using screen-printed carbon electrodes modified with gold nanoparticles and graphene oxide. *Talanta* **2017**, *175*, 331–337. [[CrossRef](#)]
42. Ramaraj, S.; Sakthivel, M.; Chen, S.-M.; Elshikh, M.S.; Chen, T.-W.; Yu, M.-C.; Ho, K.-C. Electrochemical sensing of anti-inflammatory agent in paramedical sample based on FeMoSe₂ modified SPCE: Comparison of various preparation methods and morphological effects. *Anal. Chim. Acta* **2019**, *1083*, 88–100. [[CrossRef](#)] [[PubMed](#)]
43. Mirceski, V.; Skrzypek, S.; Stojanov, L. Square-wave voltammetry. *ChemTexts* **2018**, *4*, 17. [[CrossRef](#)]
44. Mirceski, V.; Guziejewski, D.; Stojanov, L.; Gulaboski, R. Differential square-wave voltammetry. *Anal. Chem.* **2019**, *91*, 14904–14910. [[CrossRef](#)] [[PubMed](#)]
45. Mirceski, V.; Gulaboski, R.; Lovric, M.; Bogeski, I.; Kappl, R.; Hoth, M. Square-wave voltammetry: A review on the recent progress. *Electroanalysis* **2013**, *25*, 2411–2422. [[CrossRef](#)]
46. Chen, A.; Shah, B. Electrochemical sensing and biosensing based on square wave voltammetry. *Anal. Methods* **2013**, *5*, 2158–2173. [[CrossRef](#)]
47. Mirceski, V.; Gulaboski, R. Recent achievements in square-wave voltammetry (a review). *Maced. J. Chem. Chem. Eng.* **2014**, *33*, 1–12.
48. Dogan-Topal, B.; Ozkan, S.A.; Uslu, B. The analytical applications of square wave voltammetry on pharmaceutical analysis. *Open Chem. Biomed. Methods J.* **2010**, *3*, 56–73. [[CrossRef](#)]
49. Gulaboski, R.; Mirceski, V. Calculating of square-wave voltammograms—A practical on-line simulation platform. *J. Solid State Electrochem.* **2024**, *28*, 1121–1130. [[CrossRef](#)]
50. Ji, D.; Shi, Z.; Liu, Z.; Low, S.S.; Zhu, J.; Zhang, T.; Chen, Z.; Yu, X.; Lu, Y.; Lu, D. Smartphone-based square wave voltammetry system with screen-printed graphene electrodes for norepinephrine detection. *Smart Mater. Med.* **2020**, *1*, 1–9. [[CrossRef](#)]

51. Newair, E.F.; Kilmartin, P.A.; Garcia, F. Square wave voltammetric analysis of polyphenol content and antioxidant capacity of red wines using glassy carbon and disposable carbon nanotubes modified screen-printed electrodes. *Eur. Food Res. Technol.* **2018**, *244*, 1225–1237. [[CrossRef](#)]
52. Ott, C.E.; Cunha-Silva, H.; Kuberski, S.L.; Cox, J.A.; Arcos-Martínez, M.J.; Arroyo-Mora, L.E. Electrochemical detection of fentanyl with screen-printed carbon electrodes using square-wave adsorptive stripping voltammetry for forensic applications. *J. Electroanal. Chem.* **2020**, *873*, 114425. [[CrossRef](#)]
53. dos Santos Novais, A.; Arantes, L.C.; Almeida, E.S.; Rocha, R.G.; Lima, C.D.; de Almeida Melo, L.M.; Richter, E.M.; Munoz, R.A.A.; dos Santos, W.T.P.; da Silva, R.A.B. Fast on-site screening of 3, 4-methylenedioxyethylamphetamine (MDEA) in forensic samples using carbon screen-printed electrode and square wave voltammetry. *Electrochim. Acta* **2022**, *403*, 139599. [[CrossRef](#)]
54. Barsukov, Y.; Macdonald, J.R. Electrochemical impedance spectroscopy. *Charact. Mater.* **2012**, *2*, 898–913.
55. Pajkossy, T.; Jurczakowski, R. Electrochemical impedance spectroscopy in interfacial studies. *Curr. Opin. Electrochem.* **2017**, *1*, 53–58. [[CrossRef](#)]
56. Lazanas, A.C.; Prodromidis, M.I. Electrochemical impedance spectroscopy— a tutorial. *ACS Meas. Sci. Au* **2023**, *3*, 162–193. [[CrossRef](#)] [[PubMed](#)]
57. Nagles, E.; García-Beltrán, O.; Calderón, J.A. Evaluation of the usefulness of a novel electrochemical sensor in detecting uric acid and dopamine in the presence of ascorbic acid using a screen-printed carbon electrode modified with single walled carbon nanotubes and ionic liquids. *Electrochim. Acta* **2017**, *258*, 512–523. [[CrossRef](#)]
58. Chin, S.F.; Lim, L.S.; Pang, S.C.; Sum, M.S.H.; Perera, D. Carbon nanoparticle modified screen printed carbon electrode as a disposable electrochemical immunosensor strip for the detection of Japanese encephalitis virus. *Microchim. Acta* **2017**, *184*, 491–497. [[CrossRef](#)]
59. Zhang, J.; Wang, S.; Ono, K. Electrochemical impedance spectroscopy. In *Microscopy and Microanalysis for Lithium-Ion Batteries*; CRC Press: Boca Raton, FL, USA, 2023; pp. 301–350.
60. Ward, A.; Hannah, A.; Kendrick, S.; Tucker, N.; MacGregor, G.; Connolly, P. Identification and characterisation of *Staphylococcus aureus* on low cost screen printed carbon electrodes using impedance spectroscopy. *Biosens. Bioelectron.* **2018**, *110*, 65–70. [[CrossRef](#)]
61. Choi, D.Y.; Yang, J.C.; Hong, S.W.; Park, J. Molecularly imprinted polymer-based electrochemical impedimetric sensors on screen-printed carbon electrodes for the detection of trace cytokine IL-1 β . *Biosens. Bioelectron.* **2022**, *204*, 114073. [[CrossRef](#)] [[PubMed](#)]
62. Randviir, E.P. A cross examination of electron transfer rate constants for carbon screen-printed electrodes using Electrochemical Impedance Spectroscopy and cyclic voltammetry. *Electrochim. Acta* **2018**, *286*, 179–186. [[CrossRef](#)]
63. Rajendrachari, S. Investigation of Electrochemical Pitting Corrosion by Linear Sweep Voltammetry: A Fast and Robust Approach. In *Voltammetry*; Maxato, N.W., Gwebu, S.S., Hhlongo, G.H., Eds.; Intechopen: London, UK, 2019; pp. 77–91. [[CrossRef](#)]
64. Lu, W.; Xu, X.; Cole, R.B. On-line linear sweep voltammetry— electrospray mass spectrometry. *Anal. Chem.* **1997**, *69*, 2478–2484. [[CrossRef](#)] [[PubMed](#)]
65. Houam, S.; Affoune, A.M.; Atek, I.; Kesri, F.; Guermèche, R.S.; Chelaghmia, M.L.; Nacef, M.; Khelifi, O.; Banks, C.E. Determination of the standard rate constant for soluble-soluble quasi-reversible electrochemical systems by linear sweep voltammetry: Application to the electrochemical oxidation on screen-printed graphite electrodes. *Electrochim. Acta* **2023**, *449*, 142200. [[CrossRef](#)]
66. Alharthi, F.A.; Hasan, I. Screen-printed carbon electrode modified by δ -MnO₂/S@ g-C₃N₄ nanocomposite for dopamine sensing using linear sweep voltammetry. *J. Electron. Mater.* **2024**, *53*, 2115–2123. [[CrossRef](#)]
67. El Henawee, M.; Saleh, H.; Attia, A.K.; Hussien, E.M.; Derar, A.R. Carbon nanotubes bulk modified printed electrochemical sensor for green determination of vortioxetine hydrobromide by linear sweep voltammetry. *Measurement* **2021**, *177*, 109239. [[CrossRef](#)]
68. Shoub, S.A.B.; Yusof, N.A.; Hajian, R. Gold Nanoparticles/Ionophore-Modified Screen-Printed Electrode for Detection of Pb (II) in River Water Using Linear Sweep Anodic Stripping Voltammetry. *Sens. Mater.* **2017**, *29*, 555–565.
69. Ball, V. Electrodeposition of pyrogallol versus pyrocatechol using cyclic voltammetry and chronoamperometry. *J. Electroanal. Chem.* **2022**, *909*, 116142. [[CrossRef](#)]
70. Nicholas, P.; Pittson, R.; Hart, J.P. Development of a simple, low cost chronoamperometric assay for fructose based on a commercial graphite-nanoparticle modified screen-printed carbon electrode. *Food Chem.* **2018**, *241*, 122–126. [[CrossRef](#)]
71. Phasuksom, K.; Sirivat, A. Chronoamperometric detection of enzymatic glucose sensor based on doped polyindole/MWCNT composites modified onto screen-printed carbon electrode as portable sensing device for diabetes. *RSC Adv.* **2022**, *12*, 28505–28518. [[CrossRef](#)]
72. Jo, H.; Her, J.; Lee, H.; Shim, Y.-B.; Ban, C. Highly sensitive amperometric detection of cardiac troponin I using sandwich aptamers and screen-printed carbon electrodes. *Talanta* **2017**, *165*, 442–448. [[CrossRef](#)] [[PubMed](#)]
73. Barros Azeredo, N.F.; Ferreira Santos, M.S.; Sempionatto, J.R.; Wang, J.; Angnes, L. Screen-printed technologies combined with flow analysis techniques: Moving from benchtop to everywhere. *Anal. Chem.* **2021**, *94*, 250–268. [[CrossRef](#)]

74. Squizzato, A.L.; Munoz, R.A.; Banks, C.E.; Richter, E.M. An overview of recent electroanalytical applications utilizing screen-printed electrodes within flow systems. *ChemElectroChem* **2020**, *7*, 2211–2221. [\[CrossRef\]](#)
75. Marzouk, S.A.; Alyammahi, A.R.; Fanjul-Bolado, P. Development and characterization of novel flow injection, thin-layer, and batch cells for electroanalytical applications using screen-printed electrodes. *Anal. Chem.* **2021**, *93*, 16690–16699. [\[CrossRef\]](#)
76. Upan, J.; Reanpang, P.; Chailapakul, O.; Jakmunee, J. Flow injection amperometric sensor with a carbon nanotube modified screen printed electrode for determination of hydroquinone. *Talanta* **2016**, *146*, 766–771. [\[CrossRef\]](#) [\[PubMed\]](#)
77. Shih, Y.; Zen, J.-M.; Kumar, A.S.; Chen, P.-Y. Flow injection analysis of zinc pyrithione in hair care products on a cobalt phthalocyanine modified screen-printed carbon electrode. *Talanta* **2004**, *62*, 912–917. [\[CrossRef\]](#) [\[PubMed\]](#)
78. Sha, Y.; Gao, Q.; Qi, B.; Yang, X. Electropolymerization of Azure B on a screen-printed carbon electrode and its application to the determination of NADH in a flow injection analysis system. *Microchim. Acta* **2004**, *148*, 335–341. [\[CrossRef\]](#)
79. Velmurugan, M.; Thirumalraj, B.; Chen, S.-M.; Al-Hemaid, F.M.; Ali, M.A.; Elshikh, M.S. Development of electrochemical sensor for the determination of palladium ions (Pd²⁺) using flexible screen printed un-modified carbon electrode. *J. Colloid Interface Sci.* **2017**, *485*, 123–128. [\[CrossRef\]](#)
80. Gonçalves, F.D.; Rodrigues, J.A.; Ramos, R.M. Electrochemical Sensing of Vitamin D3: A Comparative Use of Glassy Carbon and Unmodified Screen-Printed Carbon Electrodes. *Chemosensors* **2023**, *11*, 575. [\[CrossRef\]](#)
81. Nawaz, M.A.H.; Majdinasab, M.; Latif, U.; Nasir, M.; Gokce, G.; Anwar, M.W.; Hayat, A. Development of a disposable electrochemical sensor for detection of cholesterol using differential pulse voltammetry. *J. Pharm. Biomed. Anal.* **2018**, *159*, 398–405. [\[CrossRef\]](#)
82. Das, A.; Sangaranarayanan, M. Electroanalytical Sensor Based on Unmodified Screen-Printed Carbon Electrode for the Determination of Levo-Thyroxine. *Electroanalysis* **2015**, *27*, 360–367. [\[CrossRef\]](#)
83. Mincu, N.-B.; Lazar, V.; Stan, D.; Mihailescu, C.M.; Iosub, R.; Mateescu, A.L. Screen-Printed Electrodes (SPE) for in vitro diagnostic purpose. *Diagnostics* **2020**, *10*, 517. [\[CrossRef\]](#)
84. Cinti, S.; Arduini, F.; Carbone, M.; Sansone, L.; Cacciotti, I.; Moscone, D.; Palleschi, G. Screen-printed electrodes modified with carbon nanomaterials: A comparison among carbon black, carbon nanotubes and graphene. *Electroanalysis* **2015**, *27*, 2230–2238. [\[CrossRef\]](#)
85. Khosrokhavar, R.; Motaharian, A.; Hosseini, M.R.M.; Mohammadsadeh, S. Screen-printed carbon electrode (SPCE) modified by molecularly imprinted polymer (MIP) nanoparticles and graphene nanosheets for determination of sertraline antidepressant drug. *Microchem. J.* **2020**, *159*, 105348. [\[CrossRef\]](#)
86. Couto, R.A.; Quinaz, M.B. Development of a Nafion/MWCNT-SPCE-based portable sensor for the voltammetric analysis of the anti-tuberculosis drug ethambutol. *Sensors* **2016**, *16*, 1015. [\[CrossRef\]](#)
87. Scala-Benuzzi, M.L.; Raba, J.; Soler-Illia, G.J.; Schneider, R.J.; Messina, G.A. Novel electrochemical paper-based immunocapture assay for the quantitative determination of ethinylestradiol in water samples. *Anal. Chem.* **2018**, *90*, 4104–4111. [\[CrossRef\]](#) [\[PubMed\]](#)
88. Madej, M.; Trzcińska, A.; Lipińska, J.; Kapica, R.; Fronczak, M.; Porada, R.; Kochana, J.; Baś, B.; Tyczkowski, J. Electrochemical sensing platform based on screen-printed carbon electrode modified with plasma polymerized acrylonitrile nanofilms for determination of bupropion. *Microchim. Acta* **2023**, *190*, 391. [\[CrossRef\]](#) [\[PubMed\]](#)
89. Suhaimi, N.F.; Baharin, S.N.A.; Jamion, N.A.; Zain, Z.M.; Sambasevam, K.P. Polyaniline-chitosan modified on screen-printed carbon electrode for the electrochemical detection of perfluorooctanoic acid. *Microchem. J.* **2023**, *188*, 108502. [\[CrossRef\]](#)
90. Karthikeyan, M.; Kumar, M.D.; Kaniraja, G.; Ananthappan, P.; Vasantha, V.S.; Karunakaran, C. Gold nanoparticles enhanced molecularly imprinted poly (3-aminophenylboronic acid) sensor for myo-inositol detection. *Microchem. J.* **2023**, *189*, 108536. [\[CrossRef\]](#)
91. Thunkhamrak, C.; Chuntib, P.; Ounnunkad, K.; Banet, P.; Aubert, P.-H.; Saianand, G.; Gopalan, A.-I.; Jakmunee, J. Highly sensitive voltammetric immunosensor for the detection of prostate specific antigen based on silver nanoprobe assisted graphene oxide modified screen printed carbon electrode. *Talanta* **2020**, *208*, 120389. [\[CrossRef\]](#)
92. Kumar, N.; Lin, Y.-J.; Huang, Y.-C.; Liao, Y.-T.; Lin, S.-P. Detection of lactate in human sweat via surface-modified, screen-printed carbon electrodes. *Talanta* **2023**, *265*, 124888. [\[CrossRef\]](#)
93. Seo, K.-D.; Hossain, M.M.; Gurudatt, N.; Choi, C.S.; Shiddiky, M.J.; Park, D.-S.; Shim, Y.-B. Microfluidic neurotransmitters sensor in blood plasma with mediator-immobilized conducting polymer/N, S-doped porous carbon composite. *Sens. Actuators B Chem.* **2020**, *313*, 128017. [\[CrossRef\]](#)
94. Ting, W.-T.; Wang, M.-J.; Howlader, M.M. Interleukin-6 electrochemical sensor using poly (o-phenylenediamine)-based molecularly imprinted polymer. *Sens. Actuators B Chem.* **2024**, *404*, 135282. [\[CrossRef\]](#)
95. Wongpakdee, T.; Crenshaw, K.; Wong, H.M.F.; de Oliveira, M.F.; Nacapracha, D.; McCord, B.R. The development of screen-printed electrodes modified with gold and copper nanostructures for analysis of gunshot residue and low explosives. *Forensic Sci. Int.* **2024**, *364*, 112243. [\[CrossRef\]](#)

96. Haddaoui, M.; Raouafi, N. Chlortoluron-induced enzymatic activity inhibition in tyrosinase/ZnO NPs/SPCE biosensor for the detection of ppb levels of herbicide. *Sens. Actuators B Chem.* **2015**, *219*, 171–178. [\[CrossRef\]](#)
97. Saengsookwaow, C.; Rangkupan, R.; Chailapakul, O.; Rodthongkum, N. Nitrogen-doped graphene–polyvinylpyrrolidone/gold nanoparticles modified electrode as a novel hydrazine sensor. *Sens. Actuators B Chem.* **2016**, *227*, 524–532. [\[CrossRef\]](#)
98. Durai, L.; Badhulika, S. Ultra-selective, trace level detection of As³⁺ ions in blood samples using PANI coated BiVO₄ modified SPCE via differential pulse anode stripping voltammetry. *Mater. Sci. Eng. C* **2020**, *111*, 110806. [\[CrossRef\]](#) [\[PubMed\]](#)
99. Jin, M.; Zhang, X.; Zhen, Q.; He, Y.; Chen, X.; Lyu, W.; Han, R.; Ding, M. An electrochemical sensor for indole in plasma based on MWCNTs-chitosan modified screen-printed carbon electrode. *Biosens. Bioelectron.* **2017**, *98*, 392–397. [\[CrossRef\]](#)
100. Zhou, L. Molecularly imprinted sensor based on Ag-Au NPs/SPCE for lactate determination in sweat for healthcare and sport monitoring. *Int. J. Electrochem. Sci.* **2021**, *16*, 211043. [\[CrossRef\]](#)
101. Zuliska, S.; Zakkiyah, S.N.; Hartati, Y.W.; Einaga, Y.; Maksun, I.P. Electrochemical aptasensor for ultrasensitive detection of glycated hemoglobin (HbA1c) using gold-modified SPCE. *Sens. Bio-Sens. Res.* **2025**, *47*, 100765. [\[CrossRef\]](#)
102. Thangphatthanarunguang, J.; Pasakon, P.; Wisitsoraat, A.; Tuantranont, A.; Intasanta, V.; Karuwan, C. Facile surface modification of the poly (L-cysteine) on 2D-printed reduced graphene oxide electrode to fabricate a highly sensitive electrochemical sensor for determining the antipsychotic drug olanzapine. *Surf. Interfaces* **2024**, *46*, 104145. [\[CrossRef\]](#)
103. Hayat, A.; Haider, W.; Rolland, M.; Marty, J.-L. Electrochemical grafting of long spacer arms of hexamethyldiamine on a screen printed carbon electrode surface: Application in target induced ochratoxin A electrochemical aptasensor. *Analyst* **2013**, *138*, 2951–2957. [\[CrossRef\]](#)
104. Hue, N.T.; Pham, T.N.; Dinh, N.X.; Van Tuan, H.; Thuy, N.T.T.; Nam, M.H.; Lam, V.D.; Le, A.-T.; Huy, T.Q. AuNPs-modified screen-printed electrodes (SPCE and SPPtE) for enhanced direct detection of chloramphenicol. *J. Electron. Mater.* **2022**, *51*, 1669–1680. [\[CrossRef\]](#)
105. Kim, J.; Kim, H.; Han, G.H.; Hong, S.; Park, J.; Bang, J.; Kim, S.Y.; Ahn, S.H. Electrodeposition: An efficient method to fabricate self-supported electrodes for electrochemical energy conversion systems. *Exploration* **2022**, *2*, 20210077. [\[CrossRef\]](#) [\[PubMed\]](#)
106. Zangari, G. Electrodeposition of alloys and compounds in the era of microelectronics and energy conversion technology. *Coatings* **2015**, *5*, 195–218. [\[CrossRef\]](#)
107. Borges, J.; Mano, J.F. Molecular interactions driving the layer-by-layer assembly of multilayers. *Chem. Rev.* **2014**, *114*, 8883–8942. [\[CrossRef\]](#)
108. Richardson, J.J.; Cui, J.; Bjornmalm, M.; Braunger, J.A.; Ejima, H.; Caruso, F. Innovation in layer-by-layer assembly. *Chem. Rev.* **2016**, *116*, 14828–14867. [\[CrossRef\]](#) [\[PubMed\]](#)
109. Xiao, F.-X.; Pagliaro, M.; Xu, Y.-J.; Liu, B. Layer-by-layer assembly of versatile nanoarchitectures with diverse dimensionality: A new perspective for rational construction of multilayer assemblies. *Chem. Soc. Rev.* **2016**, *45*, 3088–3121. [\[CrossRef\]](#)
110. Pundir, C.S.; Devi, R. Biosensing methods for xanthine determination: A review. *Enzym. Microb. Technol.* **2014**, *57*, 55–62. [\[CrossRef\]](#)
111. Mandoj, F.; Nardis, S.; Di Natale, C.; Paolesse, R. Porphyrinoid thin films for chemical sensing. In *Encyclopedia of Interfacial Chemistry: Surface Science and Electrochemistry*; Elsevier: Amsterdam, The Netherlands, 2018; pp. 422–443.
112. Friebe, C.; Hager, M.D.; Winter, A.; Schubert, U.S. Metal-containing polymers via electropolymerization. *Adv. Mater.* **2012**, *24*, 332–345. [\[CrossRef\]](#)
113. Wang, J.; Chen, X.; Reis, R.; Chen, Z.; Milne, N.; Winther-Jensen, B.; Kong, L.; Dumée, L.F. Plasma modification and synthesis of membrane materials—A mechanistic review. *Membranes* **2018**, *8*, 56. [\[CrossRef\]](#)
114. Ye, Z.; Zhao, L.; Nikiforov, A.; Giraudon, J.-M.; Chen, Y.; Wang, J.; Tu, X. A review of the advances in catalyst modification using nonthermal plasma: Process, Mechanism and Applications. *Adv. Colloid Interface Sci.* **2022**, *308*, 102755. [\[CrossRef\]](#) [\[PubMed\]](#)
115. Tyona, M. A theoretical study on spin coating technique. *Adv. Mater. Res.* **2013**, *2*, 195. [\[CrossRef\]](#)
116. Mustafa, H.A.M.; Jameel, D.A. Modeling and the main stages of spin coating process: A review. *J. Appl. Sci. Technol. Trends* **2021**, *2*, 119–123. [\[CrossRef\]](#)
117. Aziz, F.; Ismail, A.F. Spray coating methods for polymer solar cells fabrication: A review. *Mater. Sci. Semicond. Process.* **2015**, *39*, 416–425. [\[CrossRef\]](#)
118. Frederichi, D.; Scialante, M.H.N.O.; Bergamasco, R. Structured photocatalytic systems: Photocatalytic coatings on low-cost structures for treatment of water contaminated with micropollutants—A short review. *Environ. Sci. Pollut. Res.* **2021**, *28*, 23610–23633. [\[CrossRef\]](#)
119. Kumar, A.K.S.; Zhang, Y.; Li, D.; Compton, R.G. A mini-review: How reliable is the drop casting technique? *Electrochem. Commun.* **2020**, *121*, 106867. [\[CrossRef\]](#)
120. Zhao, C.; Xing, L.; Xiang, J.; Cui, L.; Jiao, J.; Sai, H.; Li, Z.; Li, F. Formation of uniform reduced graphene oxide films on modified PET substrates using drop-casting method. *Particuology* **2014**, *17*, 66–73. [\[CrossRef\]](#)
121. Eslamian, M.; Soltani-Kordshuli, F. Development of multiple-droplet drop-casting method for the fabrication of coatings and thin solid films. *J. Coat. Technol. Res.* **2018**, *15*, 271–280. [\[CrossRef\]](#)

122. Kava, A.A.; Henry, C.S. Exploring carbon particle type and plasma treatment to improve electrochemical properties of stencil-printed carbon electrodes. *Talanta* **2021**, *221*, 121553. [\[CrossRef\]](#)
123. Oliveira, I.G.; Gallina, F.C.; da Silva, A.P.; da Silva, A.C.; Júnior, F.E.B.; de Carvalho, A.E.; Lanza, M.R.; Martelli, S.M.; Barros, W.R. Disposable and flexible screen-printed-carbon electrode modified with Au/poly-beta-cyclodextrin as electrochemical platform for estriol detection. *Microchem. J.* **2024**, *206*, 111521. [\[CrossRef\]](#)
124. Osaki, S.; Saito, M.; Nagai, H.; Tamiya, E. Surface Modification of Screen-Printed Carbon Electrode through Oxygen Plasma to Enhance Biosensor Sensitivity. *Biosensors* **2024**, *14*, 165. [\[CrossRef\]](#)
125. Pillai, R.R.; Adhikari, K.R.; Gardner, S.; Sunilkumar, S.; Sanas, S.; Mohammad, H.; Thomas, V. Inkjet-printed plasma-functionalized polymer-based capacitive sensor for PAHs. *Mater. Today Commun.* **2023**, *35*, 105659. [\[CrossRef\]](#)
126. Pereira, J.F.; Rocha, R.G.; Castro, S.V.; Joao, A.F.; Borges, P.H.; Rocha, D.P.; de Siervo, A.; Richter, E.M.; Nossol, E.; Gelamo, R.V. Reactive oxygen plasma treatment of 3D-printed carbon electrodes towards high-performance electrochemical sensors. *Sens. Actuators B Chem.* **2021**, *347*, 130651. [\[CrossRef\]](#)
127. Chang, Y.-H.; Hsu, C.-L.; Yuan, C.-J.; Tang, S.-F.; Chiang, H.-J.; Jang, H.-D.; Chang, K.-S. Improvement of the inter-electrode reproducibility of screen-printed carbon electrodes by oxygen plasma etching and an image color level method for quality control. *Mater. Sci. Eng. C* **2011**, *31*, 1265–1270. [\[CrossRef\]](#)
128. Prasad, K.S.; Muthuraman, G.; Zen, J.-M. The role of oxygen functionalities and edge plane sites on screen-printed carbon electrodes for simultaneous determination of dopamine, uric acid and ascorbic acid. *Electrochem. Commun.* **2008**, *10*, 559–563. [\[CrossRef\]](#)
129. Ghamouss, F.; Tessier, P.-Y.; Djouadi, M.; Besland, M.-P.; Boujtita, M. Examination of the electrochemical reactivity of screen printed carbon electrode treated by radio-frequency argon plasma. *Electrochem. Commun.* **2007**, *9*, 1798–1804. [\[CrossRef\]](#)
130. Kanyong, P.; Rawlinson, S.; Davis, J. Gold nanoparticle modified screen-printed carbon arrays for the simultaneous electrochemical analysis of lead and copper in tap water. *Microchim. Acta* **2016**, *183*, 2361–2368. [\[CrossRef\]](#)
131. Syafira, R.S.; Devi, M.J.; Gaffar, S.; Irkham; Kurnia, I.; Arnafia, W.; Einaga, Y.; Syakir, N.; Noviyanti, A.R.; Hartati, Y.W. Hydroxyapatite-gold modified screen-printed carbon electrode for selective SARS-CoV-2 antibody immunosensor. *ACS Appl. Bio Mater.* **2024**, *7*, 950–960. [\[CrossRef\]](#)
132. Zakiyyah, S.N.; Satriana, N.P.; Fransisca, N.; Gaffar, S.; Syakir, N.; Irkham, I.; Hartati, Y.W. Gold nanoparticle-modified screen-printed carbon electrodes for label-free detection of SARS-CoV-2 RNA using drop casting and spray coating methods. *ADMET DMPK* **2025**, *13*, 2577. [\[CrossRef\]](#) [\[PubMed\]](#)
133. Wang, W.; Yi, Z.; Liang, Q.; Zhen, J.; Wang, R.; Li, M.; Zeng, L.; Li, Y. In situ deposition of gold nanoparticles and L-Cysteine on screen-printed carbon electrode for rapid electrochemical determination of As (III) in water and tea. *Biosensors* **2023**, *13*, 130. [\[CrossRef\]](#) [\[PubMed\]](#)
134. Eissa, S.; Alshehri, N.; Rahman, A.M.A.; Dasouki, M.; Abu-Salah, K.M.; Zourob, M. Electrochemical immunosensors for the detection of survival motor neuron (SMN) protein using different carbon nanomaterials-modified electrodes. *Biosens. Bioelectron.* **2018**, *101*, 282–289. [\[CrossRef\]](#) [\[PubMed\]](#)
135. Magar, H.S.; Hassan, R.Y.; Abbas, M.N. Non-enzymatic disposable electrochemical sensors based on CuO/Co₃O₄@MWCNTs nanocomposite modified screen-printed electrode for the direct determination of urea. *Sci. Rep.* **2023**, *13*, 2034. [\[CrossRef\]](#)
136. Chang, J.-L.; Chang, K.-H.; Hu, C.-C.; Cheng, W.-L.; Zen, J.-M. Improved voltammetric peak separation and sensitivity of uric acid and ascorbic acid at nanoplatelets of graphitic oxide. *Electrochem. Commun.* **2010**, *12*, 596–599. [\[CrossRef\]](#)
137. Ahmad, K.; Kim, H. Fabrication of nitrogen-doped reduced graphene oxide modified screen printed carbon electrode (N-rGO/SPCE) as hydrogen peroxide sensor. *Nanomaterials* **2022**, *12*, 2443. [\[CrossRef\]](#)
138. Pan, M.; Guo, P.; Liu, H.; Lu, J.; Xie, Q. Graphene oxide modified screen-printed electrode for highly sensitive and selective electrochemical detection of ciprofloxacin residues in milk. *J. Anal. Sci. Technol.* **2021**, *12*, 55. [\[CrossRef\]](#)
139. Viet, N.X.; Hoan, N.X.; Takamura, Y. Development of highly sensitive electrochemical immunosensor based on single-walled carbon nanotube modified screen-printed carbon electrode. *Mater. Chem. Phys.* **2019**, *227*, 123–129. [\[CrossRef\]](#)
140. Chuntib, P.; Themsirimongkon, S.; Saipanya, S.; Jakmunee, J. Sequential injection differential pulse voltammetric method based on screen printed carbon electrode modified with carbon nanotube/Nafion for sensitive determination of paraquat. *Talanta* **2017**, *170*, 1–8. [\[CrossRef\]](#)
141. Sadeghi, S.; Garmroodi, A. Sensitive detection of sulfasalazine at screen printed carbon electrode modified with functionalized multiwalled carbon nanotubes. *J. Electroanal. Chem.* **2014**, *727*, 171–178. [\[CrossRef\]](#)
142. Hu, Z.; Yang, L.; Yang, W.; Han, J.; Li, C.; Liu, Q.; Xiang, Z.; Wu, J. The Construction and Mechanism of SPCE/Cu₂O@MWCNTs Electrochemical Sensor for Menthone Detection for Epileptic Seizures Prediction. *Adv. Healthc. Mater.* **2025**, *14*, 2500764. [\[CrossRef\]](#) [\[PubMed\]](#)
143. Araujo, D.A.; Camargo, J.R.; Pradela-Filho, L.A.; Lima, A.P.; Munoz, R.A.; Takeuchi, R.M.; Janegitz, B.C.; Santos, A.L. A lab-made screen-printed electrode as a platform to study the effect of the size and functionalization of carbon nanotubes on the voltammetric determination of caffeic acid. *Microchem. J.* **2020**, *158*, 105297. [\[CrossRef\]](#)

144. Fried, J.R. *Polymer Science and Technology*; Pearson Education: London, UK, 2014.
145. Awuzie, C.I. Conducting polymers. *Mater. Today Proc.* **2017**, *4*, 5721–5726. [[CrossRef](#)]
146. Das, T.K.; Prusty, S. Review on conducting polymers and their applications. *Polym.-Plast. Technol. Eng.* **2012**, *51*, 1487–1500. [[CrossRef](#)]
147. Šišoláková, I.; Gorejová, R.; Chovancová, F.; Shepa, J.; Ngwabebhoh, F.A.; Fedorková, A.S.; Sáha, P.; Oriňáková, R. Polymer-based electrochemical sensor: Fast, accurate, and simple insulin diagnostics tool. *Electrocatalysis* **2023**, *14*, 697–707. [[CrossRef](#)]
148. Raj, M.; Gupta, P.; Goyal, R.N.; Shim, Y.-B. Graphene/conducting polymer nano-composite loaded screen printed carbon sensor for simultaneous determination of dopamine and 5-hydroxytryptamine. *Sens. Actuators B Chem.* **2017**, *239*, 993–1002. [[CrossRef](#)]
149. Filik, H.; Avan, A.A. Conducting polymer modified screen-printed carbon electrode coupled with magnetic solid phase microextraction for determination of caffeine. *Food Chem.* **2018**, *242*, 301–307. [[CrossRef](#)]
150. BelBruno, J.J. Molecularly imprinted polymers. *Chem. Rev.* **2018**, *119*, 94–119. [[CrossRef](#)] [[PubMed](#)]
151. Dong, J.; Zhang, H.; Ding, Z.; Li, J.; Xu, L.; Kong, Y.; Zheng, G. An electrochemical sensor based on molecularly imprinted poly (o-phenylenediamine) for the detection of thymol. *Anal. Biochem.* **2024**, *691*, 115551. [[CrossRef](#)]
152. Song, Z.; Yin, M.; Rui, B.; Liu, T.; Song, W.; Sun, L.; Li, S.; Wang, J.; Han, M.; Gou, G. A novel molecularly imprinted polymer sensor for sweat cortisol with embedded probe based on the co-deposition of Prussian Blue and Polypyrrole. *Sens. Actuators Rep.* **2024**, *8*, 100217. [[CrossRef](#)]
153. Stoica, B.E.; Gavrilă, A.-M.; Sarbu, A.; Iovu, H.; Brisset, H.; Miron, A.; Iordache, T.-V. Uncovering the behavior of screen-printed carbon electrodes modified with polymers molecularly imprinted with lipopolysaccharide. *Electrochem. Commun.* **2021**, *124*, 106965. [[CrossRef](#)]
154. Mohsenzadeh, E.; Ratautaite, V.; Brazys, E.; Ramanavicius, S.; Zukauskas, S.; Plausinaitis, D.; Ramanavicius, A. Design of molecularly imprinted polymers (MIP) using computational methods: A review of strategies and approaches. *Wiley Interdiscip. Rev. Comput. Mol. Sci.* **2024**, *14*, e1713. [[CrossRef](#)]
155. Ebrahimi, F. *Nanocomposites: New Trends and Developments*; BoD—Books on Demand: Norderstedt, Germany, 2012.
156. Bogue, R. Nanocomposites: A review of technology and applications. *Assem. Autom.* **2011**, *31*, 106–112. [[CrossRef](#)]
157. Omanović-Miklićanin, E.; Badnjević, A.; Kazlagic, A.; Hajlovac, M. Nanocomposites: A brief review. *Health Technol.* **2020**, *10*, 51–59. [[CrossRef](#)]
158. Okpala, C.C. Nanocomposites—an overview. *Int. J. Eng. Res. Dev* **2013**, *8*, 17.
159. Okpala, C.C. The benefits and applications of nanocomposites. *Int. J. Adv. Eng. Tech* **2014**, *12*, 18.
160. Ibáñez-Redín, G.; Wilson, D.; Gonçalves, D.; Oliveira, O., Jr. Low-cost screen-printed electrodes based on electrochemically reduced graphene oxide-carbon black nanocomposites for dopamine, epinephrine and paracetamol detection. *J. Colloid Interface Sci.* **2018**, *515*, 101–108. [[CrossRef](#)]
161. Wu, Y.; Zhang, T.; Su, L.; Wu, X. Electrodeposited rGO/AuNP/MnO₂ Nanocomposite-Modified Screen-Printed Carbon Electrode for Sensitive Electrochemical Sensing of Arsenic (III) in Water. *Biosensors* **2023**, *13*, 563. [[CrossRef](#)] [[PubMed](#)]
162. Calvo, A.S.; Botas, C.; Martín-Yerga, D.; Alvarez, P.; Menéndez, R.; Costa-Garcia, A. Comparative study of screen-printed electrodes modified with graphene oxides reduced by a constant current. *J. Electrochem. Soc.* **2015**, *162*, B282. [[CrossRef](#)]
163. Adarakatti, P.S.; Foster, C.W.; Banks, C.E.; Kumar, A.N.S.; Malingappa, P. Calixarene bulk modified screen-printed electrodes (SPCCEs) as a one-shot disposable sensor for the simultaneous detection of lead(II), copper(II), and mercury(II) ions: Application to environmental samples. *Sens. Act. A* **2017**, *267*, 517–525. [[CrossRef](#)]
164. Yildiz, C.; Bayraktepe, D.E.; Yazan, Z. Highly sensitive direct simultaneous determination of zinc(II), cadmium(II), lead(II), and copper(II) based on in-situ-bismuth and merucry thin-film plated screen-printed carbon electrode. *Monatshefte Fur Chem.-Chem. Mon.* **2021**, *152*, 1527–1537. [[CrossRef](#)]
165. Kunpatee, K.; Kaewdorn, K.; Duangtong, J.; Chaiyo, S.; Chailapakul, O.; Kalcher, K.; Kerr, M.; Samphao, A. A new disposable electrochemical sensor for the individual and simultaneous determination of carbamate pesticides using a nanocomposite modified screen-printed electrode. *Microchem. J.* **2022**, *177*, 107318. [[CrossRef](#)]
166. Sgobbi, L.F.; Razzino, C.A.; Machado, S.A.S. A disposable electrochemical sensor for simultaneous detection of sulfamethoxazole and trimethoprim antibiotics in urine based on multiwalled nanotubes decorated with Prussian blue nanocubes modified screen-printed electrodes. *Electrochim. Acta* **2016**, *191*, 1010–1017. [[CrossRef](#)]
167. Al borhani, W.; Rhouati, A.; Cialla-May, D.; Popp, J.; Zourob, M. Multiplex electrochemical aptasensor for the simultaneous detection of linomycin and newmycin antibiotics. *Talanta* **2025**, *282*, 126922. [[CrossRef](#)]
168. Wu, J.; Yan, F.; Tang, J.; Zhai, C.; Ju, H. A disposable multianalyte electrochemical immunosensor array for automated simultaneous determination of tumor markers. *Clin. Chem.* **2007**, *53*, 1495–1502. [[CrossRef](#)]
169. Lai, G.; Wang, L.; Wu, J.; Ju, H.; Yan, F. Electrochemical stripping analysis of nanogold label-induced silver deposition for ultrasensitive multiplexed detection of tumor markers. *Anal. Chem. Acta.* **2012**, *721*, 1–6. [[CrossRef](#)]

170. Tabrizi, M.A.; Shamsipur, M.; Saber, R.; Sarkar, S. Simultaneous determination of CYC and VEGF165 tumor markers based on immobilization of flavin adenine dinucleotide and thionine as probes on reduced graphene oxide-poly(amidoamine)/gold nanocomposite modified dual working screen-printed electrode. *Sens. Actuat. B* **2017**, *240*, 1174–1181. [\[CrossRef\]](#)
171. Pakchin, P.S.; Nakhjavani, S.A.; Saber, R.; Ghanbari, H.; Omid, Y. Recent advances in simultaneous electrochemical multi-analyte sensing platforms. *Trends Anal. Chem.* **2017**, *92*, 32–41. [\[CrossRef\]](#)
172. Marques, R.C.B.; Costa-Rama, E.; Viswanathan, S.; Nouws, H.P.A.; Costa-García, A.; Delerue-Matos, C.; Gonzalez-García, M.B. Voltammetric immunosensor for the simultaneous analysis of the breast cancer biomarkers CA 15-3 and HER2-ECD. *Sens. Actuat. B* **2018**, *255*, 918–925. [\[CrossRef\]](#)
173. Valverde, A.; Serafin, V.; Garoz, J.; Montero-Calle, A.; Gonzáles-Cortés, A.; Arenas, C.; Camps, J.; Barderas, R.; Yañez-Sedeño, P.; Campuzano, S.; et al. Electrochemical immunoplatfrom to improve the reliability of breast cancer diagnosis through the simultaneous determination of RANKL and TNF in serum. *Sens. Actuat. B* **2020**, *314*, 128096. [\[CrossRef\]](#)
174. Torrente-Rodriguez, R.M.; Campuzano, S.; Montiel, R.-V.; Gamella, M.; Pingarron, J.M. Electrochemical bioplatfroms for the simultaneous determination of interleukin(IL)-8 and mRA and IL-8 protein oral cancer biomarkers in raw saliva. *Biosens. Bioelectron.* **2016**, *77*, 543–548. [\[CrossRef\]](#)
175. Kovarova, A.; Kastrati, G.; Pekarkova, J.; Metelka, R.; Drbohlavova, J.; Bilkova, Z.; Selesovska, R.; Korecka, L. Biosensor with electrochemically active nanocomposites for signal amplification and simultaneous detection of three ovarian cancer biomarkers. *Electrochim. Acta* **2023**, *469*, 143213. [\[CrossRef\]](#)
176. Verma, D.; Dubey, N.; Yadav, A.K.; Saraya, A.; Sharma, R.; Solanki, P.R. Disposable paper-based screen-printed electrochemical immunoplatfrom for dual detection of esophageal cancer biomarkers in patients' serum samples. *Mater. Adv.* **2024**, *5*, 2153–2168. [\[CrossRef\]](#)
177. Lee, K.; Ha, S.M.; Gurudat, N.G.; Heo, W.; Hyun, K.A.; Kim, J.; Jung, H. Machine learning-powered electrochemical aptasensor for simultaneous monitoring of di(2-ethylhexyl) phthalate and bisphenol A in variable pH environments. *J. Hazard Mater.* **2024**, *462*, 132775. [\[CrossRef\]](#) [\[PubMed\]](#)
178. de Araujo Andreotti, I.A.; Orzari, L.O.; Camargo, J.R.; Faria, R.C.; Marcolino-Junior, L.H.; Bergamini, M.F.; Gatti, A.; Janegitz, B.C. Disposable and flexible electrochemical sensor made by recyclable material and low cost conductive ink. *J. Electroanal. Chem.* **2019**, *840*, 109–116. [\[CrossRef\]](#)
179. Bhimaraya, K.; Manjunatha, J.G.; Moulya, K.P.; Tighezza, A.M.; Albaqami, M.D.; Sillanpää, M. Detection of levofloxacin using a simple and green electrochemically polymerized glycine layered carbon paste electrode. *Chemosensors* **2023**, *11*, 191. [\[CrossRef\]](#)
180. Gomes, N.O.; Paschoalin, R.T.; Bilatto, S.; Sorigotti, A.R.; Farinas, C.S.; Mattoso, L.H.C.; Machado, S.A.; Oliveira, O.N., Jr.; Raymundo-Pereira, P.A. Flexible, bifunctional sensing platform made with biodegradable mats for detecting glucose in urine. *ACS Sustain. Chem. Eng.* **2023**, *11*, 2209–2218. [\[CrossRef\]](#)
181. Gomes, N.O.; Teixeira, S.C.; Calegari, M.L.; Machado, S.A.S.; Ferreira Soares, N.F.; de Oliveira, T.V.; Raymundo-Pereira, P.A. Flexible and sustainable printed sensor strips for on-site, fast decentralized self-testing of urinary biomarkers integrated with a portable wireless analyzer. *Chem. Engineer. J.* **2023**, *472*, 14477. [\[CrossRef\]](#)
182. Janus, K.A.; Zach, M.; Achtsnicht, S.; Drinic, A.; Kopp, A.; Keusgen, M.; Schöning, M.J. Modification of a bioabsorbable carbon electrode on silk-fibroin carriers: Setting the composition and adjustment of the working potential. *Sens. Diagn.* **2025**, *4*, 353–362. [\[CrossRef\]](#)
183. Szałapak, J.; Zdanikowski, B.; Kądziela, A.; Lepak-Kuc, S.; Dybowska-Sarapuk, Ł.; Janczak, D.; Raczyński, T.; Jakubowska, M. Carbon-based composites with biodegradable matrix for flexible paper electronics. *Polymers* **2024**, *16*, 686. [\[CrossRef\]](#)
184. Kumar, A.; Maiti, P. Paper-based sustainable biosensors. *Mater. Adv.* **2024**, *5*, 3563–3586. [\[CrossRef\]](#)
185. Lawrence, C.S.K.; Tan, S.N.; Floresca, C.Z. A “green” cellulose paper based glucose amperometric biosensor. *Sens. Actuat. B* **2014**, *193*, 536–554. [\[CrossRef\]](#)
186. Santos Oliveira, R.; Burger Veríssimo de Oliveira, W.; Cunha de Souza, C.; Mendes Fernandes, B.L.; Costa Matos, M.A.; Pedrosa Lisboa, T.; Camargo Matos, R. Composite Material from Waste ABS 3D Filaments and Graphite: A Cost-Effective and Sustainable Alternative for Electrochemical Sensor Manufacturing and Voltammetric Analysis of Acebutolol. *ChemistrySelect* **2024**, *9*, e202402782. [\[CrossRef\]](#)
187. Sharma, R.; Sahoo, J.; Gandhi, S. Sustainable and Eco-Friendly 3D-Printed Electrochemical Sensors. In *Additively Manufactured Electrochemical Sensors*; Manjunatha, J.G., Hussain, C.M., Eds.; Wiley Online Library: Hoboken, NJ, USA, 2025; pp. 369–400. [\[CrossRef\]](#)
188. Cao, W.; Nie, J.; Cao, Y.; Gao, C.; Wang, M.; Lu, X.; Ma, X.; Zhang, P. A review of how to improve Ti₃C₂T_x MXene stability. *Chem. Eng. J.* **2024**, *496*, 154097. [\[CrossRef\]](#)
189. Lu, H.; Wang, J.; Wu, Z.; Yang, M.; Zhou, W.; Li, Y.; Li, H.; Zhang, Y.; Yang, J.; Yu, G.; et al. Constructing an electrochemical sensor with screen-printed electrodes incorporating Ti₃C₂T_x-PDA-AgNPs for lactate detection in sweat. *Talanta* **2025**, *285*, 127423. [\[CrossRef\]](#) [\[PubMed\]](#)

190. Parilla, M.; Detamornat, U.; Dominguez-Robles, J.; Donnelly, R.F.; De Wael, K. Wearable hollow microneedle sensing patches for the transdermal electrochemical monitoring of glucose. *Talanta* **2022**, *249*, 123695. [[CrossRef](#)] [[PubMed](#)]
191. Khosravi, S.; Soltanian, S.; Servati, A.; Khademhosseini, A.; Zu, Y.; Servati, P. Screen-printed textile-based electrochemical biosensor for noninvasive monitoring of glucose in sweat. *Biosensors* **2023**, *13*, 684. [[CrossRef](#)] [[PubMed](#)]

Disclaimer/Publisher's Note: The statements, opinions and data contained in all publications are solely those of the individual author(s) and contributor(s) and not of MDPI and/or the editor(s). MDPI and/or the editor(s) disclaim responsibility for any injury to people or property resulting from any ideas, methods, instructions or products referred to in the content.